

ECONOMIC GEOLOGY
RESEARCH UNIT

University of the Witwatersrand
Johannesburg

THE ORIGIN OF FLUIDS AND THE EFFECTS
OF METAMORPHISM ON THE PRIMARY CHEMICAL
COMPOSITIONS OF BARBERTON KOMATITES:
NEW EVIDENCE FROM GEOCHEMICAL (REE)
AND ISOTOPIC (Nd, O, H, $^{39}\text{Ar}/^{40}\text{Ar}$) DATA

C. LÉCUYER, G. GRUAU, C.R. ANHAEUSSER
and S. FOURCADE

INFORMATION CIRCULAR No. 272

UNIVERSITY OF THE WITWATERSRAND
JOHANNESBURG

THE ORIGIN OF FLUIDS AND THE EFFECTS OF METAMORPHISM
ON THE PRIMARY CHEMICAL COMPOSITIONS OF BARBERTON
KOMATHITES: NEW EVIDENCE FROM GEOCHEMICAL (REE)
AND ISOTOPIC (Nd, O, H, $^{39}\text{Ar}/^{40}\text{Ar}$) DATA

by

C. LÉCUYER*, G. GRUAU*, C.R. ANHAEUSSER** and
S. FOURCADE*

(* Laboratoire de Géochimie, Géosciences Rennes, UPR 4661 CNRS,
Institut de Géologie, Université de Rennes I, 35042 Rennes Cedex, France

** Economic Geology Research Unit, University of the Witwatersrand,
P/Bag 3, WITS 2050, Johannesburg, South Africa)

ECONOMIC GEOLOGY RESEARCH UNIT
INFORMATION CIRCULAR No. 272

December, 1993

**THE ORIGIN OF FLUIDS AND THE EFFECT OF METAMORPHISM
ON THE PRIMARY CHEMICAL COMPOSITIONS OF BARBERTON
KOMATIITES: NEW EVIDENCE FROM GEOCHEMICAL (REE)
AND ISOTOPIC (Nd, O, H, $^{39}\text{Ar}/^{40}\text{Ar}$) DATA**

ABSTRACT

Numerous greenstone relics, all containing the two lowermost formations of the Onverwacht Group, occur in the Archaean trondhjemite/tonalitic gneiss terranes south of the Barberton Greenstone Belt. In this study, we report detailed petrological, geochemical and isotopic (Nd, O, H, $^{40}\text{Ar}/^{39}\text{Ar}$) data obtained on komatiites from the Schapenburg Greenstone Remnant (SGR), the largest and best-preserved greenstone relic. The main goals are 1) to date the metamorphism affecting the SGR, using the $^{40}\text{Ar}/^{39}\text{Ar}$ dating method on amphiboles, 2) to evaluate the effect of metamorphism on the preservation of primary isotopic and chemical signatures and, 3) to estimate the temperature and water/rock ratios that prevailed during metamorphic recrystallization in order to constrain the composition and origin of the reacting fluid phase.

$^{40}\text{Ar}/^{39}\text{Ar}$ ages of 2.9 Ga obtained on two amphibole separates from the Schapenburg metavolcanics reveal the existence of a metamorphic event younger than the emplacement age (3.5 Ga). This metamorphic event belongs to a series of discrete periods of thermal activity from 3.4 to 2 Ga, each of which coincides with a major episode of magmatic activity. The ultrabasic lava flows acquired their $\delta^{18}\text{O}$ values (from +3.2 to +5‰) at high temperature ($\approx 450^\circ\text{C}$) under high water/rock ratios. The reacting water had initial isotopic values typical of metamorphic fluids ($\delta^{18}\text{O} = +5$ to +7 ‰; $\delta\text{D} = -65$ to -50‰).

REE patterns were not disturbed by metamorphic recrystallization. Despite the long time interval between emplacement and metamorphism (≈ 600 Ma), $e_{\text{Nd}}(T)$ values are uniform throughout the whole magmatic suite, indicating that the Sm-Nd system was closed on the sample scale during metamorphism. The mantle source of these greenstones was depleted in LREE as evidence by $e_{\text{Nd}}(T) \approx +2.5$.

Chemical fluxes during metamorphism were calculated for elements unfractionated by olivine removal (e.g. Na, Ca, Ti, Al and Sr), by normalizing to Nd. They suggest a significant mobility of most major elements in the cumulate zones of the lava flows. By contrast, spinifex zones appear to have preserved most of their primary chemical signatures during metamorphic recrystallization. Their $\text{CaO}/\text{Al}_2\text{O}_3$ and $\text{Al}_2\text{O}_3/\text{TiO}_2$ ratios can be used with confidence to determine the PT conditions of melting in the mantle source.

A general model of water-rock interactions applied to the sedimentary and magmatic rocks of the Onverwacht Group is also presented. The model involves conditions of metamorphism deduced from this study and available data from the literature. In addition to metavolcanic rocks, most of the oxygen isotope compositions of carbonates and cherts (except the highest values) can be explained by re-equilibration with metamorphic fluids under greenschist-amphibolite facies conditions.

____ oOo ____

THE ORIGIN OF FLUIDS AND THE EFFECTS OF METAMORPHISM
ON THE PRIMARY CHEMICAL POSITIONS OF BARBERTON
KOMATIITES: NEW EVIDENCE FROM GEOCHEMICAL (REE)
AND ISOTOPIC (Nd, O, H, $^{39}\text{Ar}/^{40}\text{Ar}$ DATA)

CONTENTS

	Page
INTRODUCTION	1
GEOLOGICAL SETTING	3
SAMPLES AND ANALYTICAL METHODS	4
RESULTS	7
Microprobe analyses of metamorphic minerals	7
Major and trace element compositions and REE patterns of whole-rock samples	7
Isotopic data	14
Neodymium	14
Oxygen and Hydrogen	14
Argon	14
DISCUSSION	17
Chemical and isotopic effect of serpentinization	20
Isotopic composition of the fluid phase	22
CONCLUDING REMARKS	24
Preservation of primary chemical and isotopic signatures during metamorphic recrystallization	24
Depleted versus undepleted mantle source	24
The Barberton Mountain Land: a window to the $\delta^{18}\text{O}$ value of the early Archaean ocean?	25
ACKNOWLEDGEMENTS	27
REFERENCES	27

____ oOo ____

Published by the Economic Geology Research Unit,
Department of Geology,
University of the Witwatersrand,
1, Jan Smuts Avenue,
Johannesburg 2001,
South Africa

ISBN 1 86838 091 2

THE ORIGIN OF FLUIDS AND THE EFFECTS OF METAMORPHISM ON THE PRIMARY CHEMICAL COMPOSITIONS OF BARBERTON KOMATIITES: NEW EVIDENCE FROM GEOCHEMICAL (REE) AND ISOTOPIC (Nd, O, H, $^{39}\text{Ar}/^{40}\text{Ar}$) DATA

INTRODUCTION

Komatiites are ultramafic volcanic rocks (MgO contents up to 30%) which occur mainly in Archaean greenstone belts. A consideration of chemical compositions, geographical distribution, and age data indicate that komatiites may provide useful constraints on the composition of the Archaean mantle (e.g. Jahn et al., 1982; Arndt, 1986a; Smith and Ludden, 1989; Gruau et al. 1990a-b). However, the invariably altered and/or metamorphosed nature of these rocks casts some doubt on their capacity to preserve primary chemical and isotopic signatures. Several authors have recently concluded that many elements, including the reputedly immobile REE, could be partly or even totally mobilized during the alteration and metamorphism of komatiites (Arndt et al., 1989; Tourpin et al., 1991; Gruau et al., 1992).

The ca. 3.5 Ga-old Onverwacht Group from the Barberton Greenstone Belt (BGB) of southern Africa (Fig. 1) contains the oldest recognizable komatiites worldwide. Komatiites from the Onverwacht Group are important for two reasons. Firstly, they represent the type locality for Al-depleted or Group II komatiites, which occur mainly in early Archaean terranes and which have lower $\text{Al}_2\text{O}_3/\text{TiO}_2$ ratios, but higher $\text{CaO}/\text{Al}_2\text{O}_3$ and $(\text{Gd}/\text{Yb})_{\text{N}}$ ratios than chondrites (e.g. Jahn et al., 1982; Arndt, 1986a; Gruau et al., 1990a). According to recent studies, the peculiar composition of these komatiites results from their formation by partial melting of deep mantle diapirs (>400 km) leaving majorite garnet as a residual phase (e.g. Gruau et al., 1990a; Herzberg, 1992). Secondly, these komatiites have initial $^{143}\text{Nd}/^{144}\text{Nd}$ ratios close to the chondritic reference ($e_{\text{Nd}}(T) \approx 0$; Hamilton et al., 1979; 1983; Gruau et al., 1990b); this feature is unusual in ancient greenstones worldwide. Other examples, such as the 3.5 Ga-old Pilbara komatiites from Western Australia, give initial $^{143}\text{Nd}/^{144}\text{Nd}$ ratios that are significantly higher than the chondritic value ($e_{\text{Nd}}(T) > 0$; see compilation in Smith and Ludden, 1989).

However, komatiites from the Onverwacht Group are not fresh rocks; they have all suffered some alteration and metamorphism. The grade of metamorphism is generally in the upper greenschist or lower amphibolite facies (e.g. Viljoen and Viljoen, 1969a). The precise context of this metamorphism remains a matter of debate. Hoffman et al. (1986) have ascribed recrystallization effects to sea-floor metamorphism on the basis of the apparent similarity between the $d^{18}\text{O}$ values of Onverwacht Group volcanic rocks and Phanerozoic ophiolites. Cloete (1991), has recently criticised this interpretation, pointing out that the actual mineral composition of pillow lavas from the Komati Formation in the Onverwacht Group is not consistent with sea-floor metamorphism. Viljoen and Viljoen (1969a) and Anhaeusser (1983), on the other hand, emphasized the role of dynamothermal contact metamorphism related to the emplacement of numerous granitic batholiths into the BGB (Fig. 1).

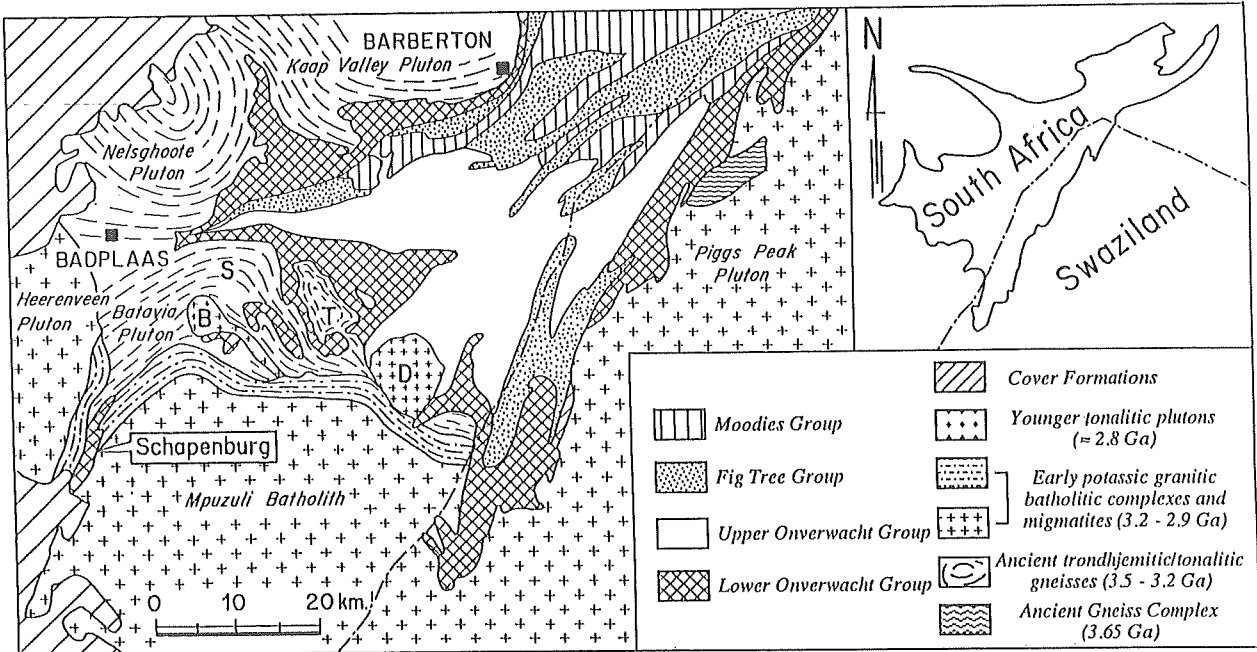


Figure 1: A simplified geological map of the southern part of the Barberton Greenstone Belt, Kaapvaal Craton, southern Africa. D: Dalmein Pluton; T: Theespruit Pluton; S: Stolzburg Pluton; B: Boesmanskop Pluton.

Several attempts have been made to date the metamorphic recrystallization event affecting the Onverwacht Group komatiites, mainly by using the $^{40}\text{Ar}/^{39}\text{Ar}$ method. Very old $^{40}\text{Ar}/^{39}\text{Ar}$ ages - in the range 3490-3450 Ma - were obtained by Lopez-Martinez et al. (1984) for a suite of peridotitic and basaltic komatiites from the type section of the Komati Formation in the Onverwacht Group. These ages are indistinguishable from the 3480-3450 Ma zircon ages which are generally thought to represent the eruption age of the Onverwacht Group komatiites (e.g. Kröner and Todt, 1988; Armstrong et al., 1990). However, Lopez-Martinez et al. (1984; 1992) have also obtained $^{40}\text{Ar}/^{39}\text{Ar}$ ages which are significantly younger: 3300-3225 Ma. Furthermore, $^{40}\text{Ar}/^{39}\text{Ar}$ ages as young as 2700 and 2100 Ma were recently reported for metasediments from the overlying Fig Tree Group (De Ronde et al., 1991). According to this study (op. cit.), the period around 2700 Ma corresponds to final granitic plutonism, and/or craton-scale deformation associated with the Limpopo orogeny.

The estimation of the $d^{18}\text{O}$ value of ancient seawater is one of the key issues of current research in earth sciences (e.g. Karhu and Epstein, 1986; Veizer et al., 1989a-b). In this respect, the Onverwacht Group komatiites are of particular interest if they contain the oxygen isotopic record of an interaction with Archaean seawater, as argued by Hoffman et al. (1986). Nevertheless, it should be borne in mind that the similarity of $d^{18}\text{O}$ values between the Onverwacht Group volcanic rocks and Phanerozoic ophiolites does not necessarily require that the reacting fluids resembled seawater. The $d^{18}\text{O}$ values of altered rocks are also a function of water/rock ratios and temperature of interaction, as well as of

the nature and relative proportions of the newly-formed mineral phases. Conditions during alteration of Phanerozoic ophiolites are not necessarily the same as those of early Archaean komatiites. Smith et al. (1984), in an investigation of the oxygen isotope compositions of Onverwacht Group volcanic rocks argued that magmatic or primitive waters ($\delta^{18}\text{O} = +7$ to $+5\text{\textperthousand}$) could have been the major fluids responsible for the hydration of the lavas at temperature of 240-450°C.

Numerous greenstone relics, all containing the two lowermost formations of the Onverwacht Group, occur in the Archaean trondhjemite/tonalitic gneiss terranes south of the BGB (e.g. Anhaeusser, 1980; Fig. 1). In the present study, we report some detailed petrological, geochemical and isotopic (Nd, O, H, $^{40}\text{Ar}/^{39}\text{Ar}$) data obtained on peridotitic and basaltic komatiites from the Schapenburg Greenstone Remnant (SGR), the largest and best-preserved greenstone relic. The aims of this work are as follows:

- 1) to determine the age of metamorphism affecting the SGR, using the $^{40}\text{Ar}/^{39}\text{Ar}$ dating method on amphiboles;
- 2) to evaluate, in relation to recent studies by Arndt et al. (1989), Tourpin et al. (1991), and Gruau et al. (1992), the effect of metamorphism on the preservation of primary isotopic and chemical signatures in some of the oldest known komatiites, and
- 3) to estimate the water/rock ratios during metamorphic recrystallization and to constrain the nature and origin of the associated fluid phase.

GEOLOGICAL SETTING

The geology of the Schapenburg Greenstone Remnant (SGR) and surrounding granite-gneiss terrane is described in detail by Anhaeusser (1983; 1991), so only a brief account is given here. The SGR, which is approximately 12 km long with a maximum width of 2.5 km, is a typical greenstone succession consisting largely of alternating volcanic and sedimentary units, and belongs to a trail of km-sized greenstone fragments that crop out within the trondhjemite/tonalitic gneisses that border the BGB (Anhaeusser and Robb, 1980; Fig. 1). In some cases, detailed mapping has revealed a lithological continuity between these fragments and the BGB (Viljoen and Viljoen, 1969b). On the basis of this observation, Viljoen and Viljoen (1969b) and Anhaeusser (1980) proposed that the greenstone lithologies found in the remnants are equivalent to the lowermost formations of the Onverwacht Group of the BGB - namely, the Sandspruit, Theespruit and Komati Formations. Recent high-precision U-Pb zircon age results for the Theespruit and overlying Komati Formations of the BGB date the deposition of the lowermost volcano-sedimentary units of the Onverwacht Group at around 3480-3450 Ma (e.g. Armstrong et al., 1990).

Extensive granitic plutonic activity is characteristic of the Barberton Mountain Land. The volumetrically dominant intrusions in the vicinity of Schapenburg are the Mpuzuli and Heerenveen batholiths (Fig. 1). These two large, sheet-like potassic plutons are equivalent to the multi-component Nelspruit batholith located further north, and all appear to have been emplaced within a short time interval around 3100 Ma ago (Kamo and Davis, 1991). Domes of trondhjemite/tonalitic gneisses (e.g. the Badplaas and Stolzburg plutons) outcrop to the

NNE (Fig. 1). They belong to the first magmatic episode defined by Anhaeusser and Robb (1981), generally yielding ages older than the Mpuzuli and Heerenveen batholiths: for example, the Stolzburg pluton is dated at 3445 ± 4 Ma by the U-Pb method on zircon (Kamo and Davis, 1991). Minor amounts of syenite were also emplaced in this area. The Boesmanskop pluton, which is located approximately 20 km NE of the SGR (Fig. 1) forms part of this suite and yielded a U-Pb zircon age of 3107 ± 1 Ma (Kamo and Davis, 1991).

The magmatic episodes involving the emplacement of granitic rocks south of the BGB were followed by other igneous and volcanic events that may have relevance to the thermal history of rocks in the SGR. Volcanic rocks forming part of the Nsuze Group crop out approximately 20 km SE of the SGR. Similar rocks, which belong to the Pongola Sequence, yielded a U-Pb zircon age of 2940 ± 22 Ma (Hegner et al., 1984). Also in this area SE of the SGR is the Usushwana Igneous Suite (UIS) comprising mainly olivine pyroxenite and gabbroic rocks. The UIS occurs as a layered dyke-like body extending from NW Swaziland into South Africa in a NW-SE direction parallel to a prominent mafic dyke swarm that extends throughout the region south of the BGB. An internal Sm-Nd isochron age of 2871 ± 30 Ma for the UIS (Hegner et al., 1984) agrees with a Rb-Sr whole-rock isochron age of 2870 ± 38 Ma obtained earlier for this suite by Davies et al. (1970). The dykes, which are mainly doleritic, have not been radiometrically dated, but the regional geology and field relationships suggest that dyke intrusion probably culminated around 1800-2400 Ma (Anhaeusser, 1983).

Volcano-sedimentary sequences in the SGR generally comprise peridotitic komatiite flows at the base (MgO contents ranging from 25 to 35%), which are overlain by basaltic komatiites ($\text{MgO} \approx 15\text{-}20\%$). Banded silicate-facies iron formations usually form the cap of each sequence. Also present in the SGR is a well-developed succession of metagreywackes and metapelites.

As commonly observed throughout the Barberton Mountain Land, rocks of the SGR have suffered pervasive alteration and metamorphism. Although some primary textures are locally preserved (e.g., spinifex in komatiite lava flows), metamorphic recrystallization has resulted in a complete obliteration of all the primary mineral assemblages. The presence of cordierite \pm staurolite assemblages, as well as the occurrence of local incipient melting in some of the metagreywackes, indicate T-P conditions between 500 and 700°C, and 2.5 and 3.5 kb for this metamorphism (Anhaeusser, 1983).

SAMPLES AND ANALYTICAL METHODS

With the aim of studying elemental mobility and fluid-rock interactions in the Schapenburg greenstones, 23 whole-rock samples - 15 peridotitic komatiites ($\text{MgO} = 26$ to 32%) and 8 basaltic komatiites ($\text{MgO} = 15$ to 20%) - were selected for geochemical (major and trace elements) and isotopic (Nd, O) analysis. Minerals separated from three of the komatiitic basalt samples (SC16, SC19, and SC20) were also analysed: amphibole for O, H, and Ar/Ar, and magnetite for O. The location of samples is given in Figure 2. Mineral proportions calculated from whole-rock chemistry and mineral compositions are presented in Table 1.

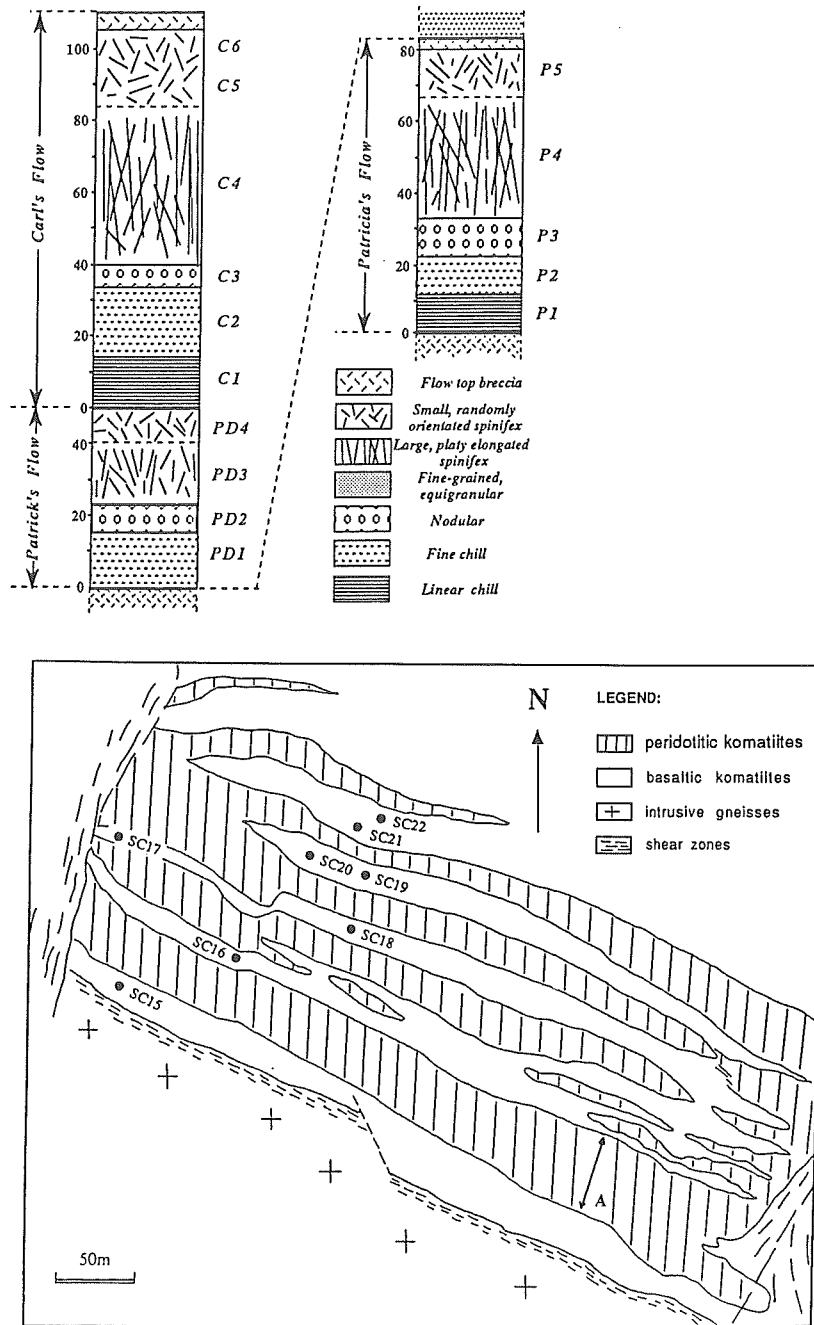


Figure 2: Sketches showing morphology, textures and volcanic structures of the three investigated komatiite flows, and sample locations. A: location of Carl's, Patrick's and Patricia's flows.

The peridotitic komatiite samples come from three superimposed spinifex-textured komatiite lava flows, the so-called Carl's Flow (samples C1 to C6), Patrick's Flow (samples PD1 to PD4) and Patricia's Flow (samples P1 to P5). Magmatic textures in these three flows are remarkably well preserved: variations in the size and shape of spinifex, for example, are still recognizable and may be mapped in detail. Furthermore, breccia zones are preserved intact at the top of Patricia's and Carl's Flows.

Table 1: Mineral composition (in weight %) of Schapenburg komatiites *

Sample N°	Serpentine	Amphibole	Chlorite	Magnetite	MSWD
<i>Carl's Flow</i>					
C1	47	33	12	7	0.41
C2	71	14	6	9	0.66
C3	47	42	6	5	0.64
C4	23	60	7	10	0.41
C5	33	53	5	9	0.51
C6	25	56	11	8	0.13
<i>Patricia's Flow</i>					
P1	70	20	1	9	0.56
P2	40	44	9	7	0.62
P3	24	63	6	8	0.40
P4	28	56	8	9	0.29
P5	29	55	7	9	0.31
<i>Patrick's Flow</i>					
PD1	70	16	4	9	0.60
PD2	26	57	10	7	0.45
PD3	32	50	9	9	0.45
PD4	24	58	9	9	0.43
<i>Basaltic komatiites</i>					
SC15	0	99	0	1	0.83
SC16	0	95	0	5	0.76
SC17	0	96	0	4	1.05
SC18	0	94	0	6	1.01
SC19	0	92	0	8	1.32
SC20	0	93	0	8	0.73
SC21	0	94	0	6	0.92
SC22	0	92	0	8	0.98

* Calculated from whole-rock and mineral major element compositions using the least-squares method of BRYAN et al. (1969). Errors are typically of the order of ± 10 to $\pm 20\%$

Mineralogically, all samples consist entirely of secondary assemblages with no relic igneous phases. In the peridotitic komatiite samples, serpentine and amphibole are the two dominant phases (up to 70 and 60 weight %, respectively; Table 1). Chlorite and magnetite also occur, but in subordinate amounts ($\leq 10\%$ each) and rare ilmenite grains are locally present. In the basaltic komatiite samples, amphibole is by far the most abundant mineral (up to 99%; Table 1), while serpentine and chlorite are absent. Minor phases are magnetite ($\leq 10\%$) and ilmenite (a few grains).

All whole-rock analyses were performed at Rennes University, except for the peridotitic komatiites which were analysed for major elements and Rb, Sr, Zr, Y, V, Ni, and Cr at the University of Witwatersrand, South Africa. Concentrations of major elements and Rb, Sr, Zr, Y, V, Ni, and Cr were determined by XRF, while the REE were analysed by the isotope dilution method. The precision is estimated at 1-5% for major elements, except for MnO (10%). For Rb, Sr, Zr, Y, V, Ni, and Cr, precisions are of the order of 10% for concentrations lower than 30 ppm. For concentrations higher than 30 ppm, the precision is 3%. Analytical errors for the REE - including chemical processing, blank effects, uncertainty in spike calibration and mass spectrometry runs - are estimated at about 5% for La and Lu, 3% for Gd and 2% for the other REE. Blanks were lower than 1 ng.

$^{143}\text{Nd}/^{144}\text{Nd}$ and $^{147}\text{Sm}/^{144}\text{Nd}$ ratios were determined following the procedure described in Gruau et al. (1987). $^{143}\text{Nd}/^{144}\text{Nd}$ ratios were measured using a single-collector TSN 206 Cameca mass spectrometer. All ratios were normalized against $^{146}\text{Nd}/^{144}\text{Nd} = 0.7219$ for isotopic fractionation effects. Results from the La Jolla Nd standard during the course of this study (35 separate runs) were $^{143}\text{Nd}/^{144}\text{Nd} = 0.511877 \pm 38$ (2s_{pop}). All measured $^{143}\text{Nd}/^{144}\text{Nd}$ ratios were thus corrected (-0.000017) to be consistent with the La Jolla reference value of 0.511860. Blanks for Nd and Sm were lower than 0.2 ng and 0.05 ng, respectively. Measured and calculated initial $^{143}\text{Nd}/^{144}\text{Nd}$ ratios are quoted throughout the text and in Table 4 in the e_{Nd} notation of Depaolo and Wasserburg (1976) as deviations in parts per 10^4 from the chondritic growth curve. The present-day $^{143}\text{Nd}/^{144}\text{Nd}$ and $^{147}\text{Sm}/^{144}\text{Nd}$ ratios for the chondritic reference reservoir are those determined by Jacobsen and Wasserburg (1980).

Oxygen was extracted using the BrF_5 method (Clayton and Mayeda, 1963) and analysed as CO_2 gas on a VG SIRA 10 mass spectrometer at Rennes University. Isotopic compositions are quoted in the standard notation relative to VSMOW. Results from the NBS28 standard gave $d^{18}\text{O} = +9.5 \pm 0.2\text{\textperthousand}$ (2s_{m}). The D/H compositions of amphiboles from samples C16, SC19 and SC20 were measured at the University of Michigan at Ann Arbor using the method of Kendall and Coplen (1985) and a Finnigan MAT delta S mass spectrometer. D/H ratios are reported in the conventional dD notation relative to VSMOW. Analyses of the NBS biotite standard gave $d\text{D} = -63 \pm 1\text{\textperthousand}$.

Microprobe analyses of minerals were performed at the IFREMER laboratory at Brest. Amphibole and magnetite separates were obtained by using conventional magnetic methods combined with handpicking. $^{40}\text{Ar}/^{39}\text{Ar}$ analyses of amphiboles from samples SC16 and SC19 were carried out at the University of Montpellier, following the procedure described in Monié et al. (1984).

RESULTS

Microprobe analyses of metamorphic minerals

Representative microprobe analyses of the metamorphic minerals, along with their structural formulae, are presented in Table 2. Structural formulae of amphiboles were calculated following the procedure of Mével (1984).

Amphibole compositions in the basaltic komatiite and peridotitic komatiite samples are not identical. In the former, the amphibole is a Mg-hornblende ($\text{Al}^{IV} \approx 0.9$; $\text{Na} + \text{K} \approx 0.4$; $\text{Mg/Mg} + \text{Fe}^{2+} \approx 0.8$). In the peridotitic komatiite samples, the amphibole shows higher $\text{Mg/Mg} + \text{Fe}^{2+}$ ratios (≈ 0.95) and lower concentrations of Al, Na and Cr (Table 2) and is a tremolite according to Leake (1978).

Chlorite analyses were normalised to 14 anhydrous oxygens, and total Fe was computed as Fe^{2+} . Chlorite, which is present only in the peridotitic komatiite samples, gives rather uniform compositions, with high $\text{Mg/Mg} + \text{Fe}^{2+}$ (0.91-0.94). The proportions of Al^{IV} and Al^{VI} are similar (≈ 1.0), suggesting crystallization under low to moderate pressure conditions (Laird, 1988). Chlorite is identified as clinochlore in the classification of Bayliss (1975). Note that the Na_2O , K_2O and CaO contents always remain very low (<0.5%; Table

Table 2: Composition of metamorphic minerals *

Sample N°	C1	C6	SC16	SC20	Sample N°	C1	C6	C6	SC16	SC20
Rock Type	peridotitic komatiite	peridotitic komatiite	basaltic komatiite	basaltic komatiite	Rock Type	peridotitic komatiite	peridotitic komatiite	komatiite ilmenite	basaltic komatiite magnetite	basaltic komatiite magnetite
Mineral	amphibole	amphibole	amphibole	amphibole	Mineral	magnetite	magnetite	ilmenite	magnetite	magnetite
SiO ₂ (%)	55.3	54.1	49.2	49.1	TiO ₂ (%)	0.17	49.6	1.76	0.49	1.89
Al ₂ O ₃	2.16	3.11	8.40	6.99	Al ₂ O ₃	2.37	1.44	1.21	1.04	4.67
TiO ₂	0.14	0.14	0.26	0.35	Cr ₂ O ₃	0.05	0.16	5.91	4.42	3.97
Cr ₂ O ₃	0.24	0.16	0.21	0.34	FeO	27.2	38.7	29.5	30.4	33.0
FeO	3.29	4.19	7.95	9.37	Fe ₂ O ₃	62.1	0.93	52.2	59.4	54.8
MnO	0.25	0.11	0.25	0.09	MnO	0.07	2.59	0.31	0.00	0.24
MgO	22.6	21.6	17.5	17.1	MgO	1.50	1.85	0.25	0.03	0.03
CaO	12.4	12.2	11.2	11.7	Total	93.4	95.2	91.1	95.7	98.6
Na ₂ O	0.59	0.78	1.44	1.53	Ti	0.04	1.93	0.44	0.12	0.45
K ₂ O	0.02	0.08	0.06	0.08	Al	0.90	0.09	0.48	0.39	1.74
Cl	0.00	0.00	0.04	0.01	Cr	0.01	0.01	1.56	1.12	0.99
Total	97.0	96.5	96.5	96.7	Fe ³⁺	15.0	0.04	13.1	14.3	12.4
					Fe ²⁺	7.30	1.68	8.23	8.11	8.37
Si	7.68	7.59	7.06	7.10	Mn	0.02	0.11	0.09	0.00	0.07
AlIV	0.32	0.41	0.94	0.90	Mg	0.72	0.14	0.12	0.01	0.01
AlVI	0.04	0.11	0.48	0.29						
Ti	0.02	0.01	0.03	0.04						
Cr	0.03	0.02	0.02	0.04						
Fe ³⁺	0.06	0.03	0.00	0.06						
Fe ²⁺	0.16	0.30	0.70	0.88						
Mn	0.03	0.01	0.03	0.01						
Mg	4.67	4.52	3.74	3.69						
Fem4	0.16	0.16	0.26	0.19						
Ca	1.84	1.84	1.72	1.81						
Na A	0.16	0.21	0.40	0.43						
K	0.00	0.01	0.01	0.01						
Mg/(Mg+Fe ²⁺) ^a	0.97	0.94	0.95	0.81						
Fe ²⁺ /Mg _a	0.03	0.07	0.05	0.24						

Table 2: (continued)

Sample N°	C1	C1	C3	C3	Sample N°	C3	C3	C3	C6
Rock Type	peridotitic komatiite	peridotitic komatiite	peridotitic komatiite	peridotitic komatiite	Rock Type	peridotitic komatiite	peridotitic komatiite	peridotitic komatiite	peridotitic komatiite
Mineral	Serpentine	Serpentine	Serpentine	Serpentine	Mineral	Chlorite	Chlorite	Chlorite	Chlorite
SiO ₂ (%)	42.2	42.9	41.4	41.4	SiO ₂ (%)	29.0	28.8	29.6	31.2
Al ₂ O ₃	1.80	1.00	0.55	0.67	Al ₂ O ₃	17.5	16.9	17.5	18.8
FeO	5.43	4.72	5.98	4.03	TiO ₂	0.06	0.07	0.04	0.01
MnO	0.22	0.05	0.08	0.00	FeO	3.92	3.96	3.70	5.03
MgO	36.3	37.4	34.9	36.4	MnO	0.00	0.00	0.01	0.09
CaO	0.04	0.00	0.00	0.01	MgO	30.5	29.4	30.4	30.2
Na ₂ O	0.01	0.01	0.01	0.04	CaO	0.03	0.00	0.01	0.05
K ₂ O	0.00	0.00	0.00	0.00	Na ₂ O	0.00	0.03	0.04	0.00
Cr ₂ O ₃	0.19	0.04	0.00	0.06	K ₂ O	0.02	0.02	0.00	0.00
Cl	0.07	0.06	0.04	n.d.	Cr ₂ O ₃	0.82	0.94	0.85	0.44
NiO	n.d.	n.d.	0.22	Cl	0.00	0.07	n.d.	0.00	0.00
Total	86.2	86.2	83.0	82.8	NiO	n.d.	n.d.	0.18	n.d.
					Total	81.8	80.2	82.3	85.9
Si	2.02	2.04	2.06	2.05	Si	2.93	2.96	2.97	3.00
Al	0.10	0.06	0.03	0.04	AlIV	1.08	1.04	1.03	1.00
Fe	0.22	0.19	0.25	0.17	AlVI	1.01	1.02	1.03	1.13
Mn	0.01	0.00	0.00	0.00	Ti	0.00	0.01	0.00	0.00
Mg	2.58	2.65	2.59	2.68	Fe	0.33	0.34	0.31	0.40
Ca	0.00	0.00	0.00	0.00	Mg	4.58	4.52	4.55	4.33
Na	0.00	0.00	0.00	0.00	Mn	0.00	0.00	0.00	0.01
K	0.00	0.00	0.00	0.00	Cr	0.07	0.08	0.07	0.03
Cr	0.01	0.00	0.00	0.94	Ca	0.00	0.00	0.00	0.01
Mg/(Mg+Fe ²⁺) ^a	0.92	0.93	0.91		Na	0.00	0.01	0.01	0.00
					K	0.00	0.00	0.00	0.00
					AlVI+2Ti+Cr-1	0.08	0.11	0.10	0.17
					Mg/(Mg+Fe ²⁺) ^a	0.93	0.93	0.94	0.92
					Fe ²⁺ /Mg ^a	0.07	0.08	0.07	0.09

^a Atom ratio

n.d.: not determined

* The compositions presented in this table are representative compositions corresponding to individual microprobe spots, not average values.
 Complete data base (about 80 analyses) can be obtained from the authors on request

2), indicating that the common problem of submicroscopic intergrowths of chlorite and other sheet silicates (ERNST, 1983) was not encountered in the present study.

Serpentine in the peridotitic komatiite samples is dominantly antigorite (X-ray diffractometry). It often contains traces of Cl (0.035-0.072 %), while Mg/(Mg+Fe) ratios are in the range 0.91-0.94 (Table 2).

Compositions of Fe-Ti oxides are rather uniform (Table 2). Magnetite and Ti-magnetite are dominant, while ilmenite is very subordinate (a few grains). TiO_2 and Cr_2O_3 contents in Ti-magnetites and magnetites reach 2% and 6%, respectively. Significant proportions of Al_2O_3 are also measured (up to \approx 5%; Table 2).

Major and trace element compositions and REE patterns of whole-rock samples

All studied samples are basic-ultrabasic rocks (Table 3). MgO contents are 14.5-19.6% in the basaltic komatiites and 25.5-31.8% in the peridotitic komatiites. Major and trace elements contents vary little in the basaltic komatiites (e.g. $\text{Al}_2\text{O}_3=5.3\text{-}6.0\%$; $\text{CaO}=9.6\text{-}12\%$; $\text{TiO}_2=0.54\text{-}0.65\%$; $\text{Zr}=40\text{-}45\text{ppm}$). In the peridotitic komatiite lava flows, concentrations are also fairly uniform (e.g. $\text{Al}_2\text{O}_3=2.5\text{-}5.1\%$; $\text{TiO}_2=0.15\text{-}0.41\%$), although samples from the upper spinifex zones generally yield lower MgO, Ni, Cr, and higher SiO_2 , CaO , Al_2O_3 , TiO_2 , Na_2O , Zr, Sr, Y, and V contents than samples from the lower zones with no spinifex. Except for some of the basaltic komatiites (e.g. SC18), the degree of hydration is generally very high (2-9%), being related to variable amounts of serpentine and chlorite (Tables 1, 2 and 3).

As can be seen in Figure 3, the $\text{Al}_2\text{O}_3/\text{TiO}_2$ and $\text{CaO}/\text{Al}_2\text{O}_3$ ratios of Schapenburg greenstones are typical of Al-depleted or Group II komatiites (Jahn et al., 1982; Gruau et al., 1990a). In the basaltic komatiites, both ratios are nearly constant ($\text{Al}_2\text{O}_3/\text{TiO}_2=1.00\pm0.7$ (1s); $\text{CaO}/\text{Al}_2\text{O}_3=1.8\pm0.1$ (1s)). In the peridotitic komatiites, distributions are more variable, samples from the base of the flows generally yielding higher $\text{Al}_2\text{O}_3/\text{TiO}_2$ (up to ≈ 17), but lower $\text{CaO}/\text{Al}_2\text{O}_3$ ratios (down to 1.1) than samples from the upper spinifex zones (Table 3; Fig. 3). Average values for the peridotitic komatiite flow samples are 12.7 ± 2.4 (1s) for $\text{Al}_2\text{O}_3/\text{TiO}_2$, and 1.6 ± 0.3 (1s) for $\text{CaO}/\text{Al}_2\text{O}_3$.

REE concentrations (Table 3; Fig. 4) were determined in 8 peridotitic komatiites (samples C1 to C6, P3, and PD3) and 4 basaltic komatiites (samples SC15, SC16, SC20, and SC21). Three important points should be underlined:

1) apart from a variable Eu anomaly ($\text{Eu}/\text{Eu}^*=0.95\text{-}1.62$), normalized patterns are remarkably similar (Fig. 4). Besides low $\text{Al}_2\text{O}_3/\text{TiO}_2$ and high $\text{CaO}/\text{Al}_2\text{O}_3$ ratios, another typical geochemical feature of Al-depleted or Group II komatiites is the existence of a systematic depletion in HREE, a feature also observed in the present sample suite. The mean value of the $(\text{Gd}/\text{Yb})_N$ ratio, a measure of the slope the HREE pattern, for Al-depleted or Group II komatiites worldwide (including samples from the type section of the Onverwacht Group in the BGB) is 1.4 ± 0.2 (1s) (JAHN et al., 1982; ARNDT, 1986a; GRUAU et al., 1990a). In the peridotitic and basaltic komatiites from Schapenburg, the mean values of this ratio are 1.64 ± 0.06 (1s) and 1.54 ± 0.04 (1s), respectively.

Table 3: Major and trace elements in Schapenburg komatiites

Sample N°	P1	P2	P3	P4	P5	PDI	PD2	PD3	FD4	C1	C2	C3	C4	C5	C6	SCI5	SCI6	SCI7	SCI8	SCI9	SCI0	SCI20	SCI21	SCI22
	Patricia's flow				Patrick's flow					Carl's flow					BK	BK	BK	BK	BK	BK	BK	BK	BK	
	LCZ	LCZ	USZ	USZ	LCZ	USZ	LCZ	USZ	LCZ	LCZ	USZ	USZ	USZ	USZ	USZ	USZ	USZ	USZ	USZ	USZ	USZ	USZ	USZ	
Major elements																								
SiO ₂ (%)	41.3	44.1	47.1	45.6	45.5	40.1	45.9	44.4	45.9	43.1	39.5	45.1	45.7	44.6	48.8	49.4	48.3	48.7	48.0	48.8	49.0			
Al ₂ O ₃	2.66	3.52	3.85	4.24	4.09	2.90	3.96	4.08	4.45	4.40	2.54	3.47	4.03	3.77	5.07	6.03	5.81	5.97	5.48	5.30	5.99			
TiO ₂	0.18	0.30	0.39	0.37	0.32	0.19	0.39	0.32	0.38	0.26	0.15	0.31	0.41	0.33	0.37	0.54	0.60	0.59	0.58	0.59	0.56	0.60		
Fe ₂ O ₃ (ΣFe)	12.6	9.9	10.7	12.3	12.3	12.8	9.88	12.0	11.7	9.86	11.7	9.38	12.3	12.2	11.9	12.2	15.4	14.8	14.9	13.7	15.5			
MnO	0.12	0.18	0.18	0.18	0.17	0.11	0.18	0.19	0.18	0.15	0.13	0.18	0.18	0.17	0.18	0.21	0.24	0.23	0.25	0.27	0.20	0.23		
MgO	31.8	28.4	26.0	26.4	31.8	26.5	27.0	26.2	30.0	31.8	29.9	25.5	26.4	25.9	19.6	17.3	15.8	14.5	18.0	18.9	15.4			
CaO	3.46	6.40	8.15	7.12	7.08	3.14	7.59	6.81	7.73	4.96	2.99	6.16	7.85	7.15	6.77	9.63	10.0	10.7	10.4	12.1	10.3	10.8		
Na ₂ O	0.10	0.28	0.51	0.48	0.47	0.14	0.42	0.40	0.49	0.13	0.03	0.21	0.47	0.41	0.36	1.18	1.29	1.39	1.55	1.40	1.27	1.30		
K ₂ O	0.05	0.06	0.07	0.07	0.08	0.05	0.08	0.07	0.07	0.05	0.05	0.05	0.05	0.07	0.07	0.07	0.07	0.07	0.07	0.11	0.07	0.09		
P ₂ O ₅	0.03	0.04	0.05	0.04	0.05	0.03	0.04	0.04	0.05	0.03	0.02	0.03	0.02	0.03	0.07	0.04	0.04	0.05	0.06	0.05	0.05	0.06		
L.O.I.	8.37	4.93	3.39	3.39	3.45	8.53	5.37	5.14	3.33	7.43	9.05	5.36	3.28	4.18	4.32	2.28	0.91	0.80	0.75	0.76	0.84	1.11	0.67	
Total	100.6	98.1	100.3	100.2	99.9	99.8	100.3	100.5	100.5	100.4	98.0	100.2	99.9	99.4	100.6	100.2	99.7	99.4	100.0	99.7	100.1	99.9		
Al ₂ O ₃ /TiO ₂	14.8	11.7	9.9	11.5	12.8	15.3	10.2	12.8	11.7	16.9	11.9	11.2	9.8	11.4	13.7	11.2	9.7	10.0	9.2	10.9	9.3	9.5	10.0	
CaO/Al ₂ O ₃	1.30	1.82	2.12	1.68	1.73	1.08	1.92	1.67	1.74	1.13	1.18	1.78	1.95	1.90	1.34	1.60	1.72	1.81	1.91	1.87	1.92	1.80		
Trace elements																								
Rb (ppm)	<2	<2	<2	<2	<2	<2	<2	<2	<2	<2	<2	<2	<2	<2	<2	<2	<2	<2	<2	<2	<1	<1	<1	
Sr	21	61	75	76	19	65	60	79	31	2	50	82	71	70	51	104	75	105	87	68	79	75		
Y	6	10	12	9	10	5	8	9	12	8	6	10	11	12	7	12	11	14	12	10	9	12		
Zr	9	16	23	17	17	9	20	22	21	14	14	32	15	20	19	16	44	42	45	41	42	40	43	
N _b	3	4	4	3	2	2	2	2	2	3	2	3	2	3	2	3	2	5	4	5	4	5		
Ni	2020	1520	1310	1330	1340	2050	1290	1480	1250	1850	2170	1640	1070	1440	1490	720	520	440	530	370	620	710	410	
Cr	1810	2500	2590	2510	2480	1880	2650	2520	2600	2150	1700	2490	2550	2300	1880	2520	1540	2560	1350	2350	2300	2300	1960	
La		1.68				1.51		1.10	0.96		1.22	1.71	1.49	1.46	3.17	2.73			2.91	2.51				
Ce		4.69				4.06		3.08	2.73		3.52	4.69	4.24	3.94	6.62	7.54			7.77	6.90				
Nd		3.68				3.29		2.42	2.14		2.85	3.65	3.30	3.25	5.47	5.62			5.78	5.20				
Sm		1.15				1.03		0.76	0.64		0.89	1.14	1.03	1.00	1.57	1.70			1.71	1.57				
Eu		0.43				0.41		0.28	0.24		0.30	0.42	0.41	0.40	0.67	0.70			0.75	0.90				
Gd		1.41				1.26		0.93	0.78		1.10	1.42	1.26	1.27	1.97	2.07			2.07	1.90				
Dy		1.44				1.32		0.96	0.78		1.14	1.42	1.29	1.27	2.05	2.15			2.15	1.98				
Er		0.78				0.73		0.53	0.44		0.64	0.78	0.73	0.71	1.20	1.21			1.24	1.11				
Yb		0.66				0.62		0.46	0.41		0.55	0.66	0.62	0.61	1.06	1.04			1.07	1.01				
Lu		0.10				0.10		0.07	0.07		0.10	0.09	0.10	0.09	0.16	0.16			0.13	0.15				
(La/Sr) _N	0.89		0.88		0.91	0.88		0.91	0.84		0.92	0.88	0.89	0.89	1.23	0.98			1.03	0.98				
(Gd/Yb) _N	1.71		1.62		1.61	1.55		1.60	1.72		1.63	1.67	1.49	1.59	1.56	1.52			1.24	1.62				
Eu/Eu*	1.04		1.12		1.03	1.05		0.95	1.03		1.10	1.10	1.10	1.10	1.18	1.18								

2) Although all the LREE patterns display a convex shape (maximum around Nd-Sm; Fig. 4), the depletion in La and Ce always remains moderate ($(La/Sm)_N = 0.92 \pm 0.06$ (1s)). A $(La/Sm)_N$ ratio close to 1.0 is common in most komatiites from Barberton (e.g. JAHN et al., 1982; GRUAU et al., 1990b), which is in marked contrast with the strong depletion of LREE generally observed elsewhere in this rock type (see Smith and Ludden, 1989, for data compilation).

3) good negative correlations are observed between the REE, and the MgO and Ni concentrations. This is true on the scale of the whole sample suite, the basaltic komatiites having absolute REE concentrations about twice those of the peridotitic komatiites with higher MgO and Ni contents. This also applies at the scale of a single flow of peridotitic komatiite: samples from Carl's Flow show a regular increase of REE contents for decreasing MgO and Ni contents (Table 3).

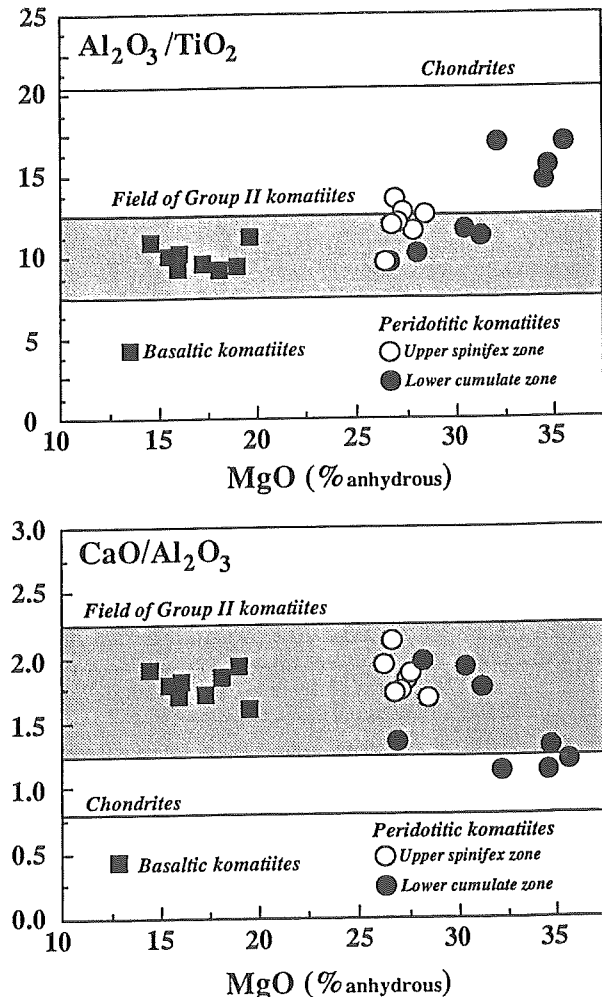


Figure 3: Al_2O_3 / TiO_2 vs. MgO and CaO / Al_2O_3 vs MgO plots. Fields of Group II komatiites are from Jahn et al. (1982) and Gruau et al. (1990).

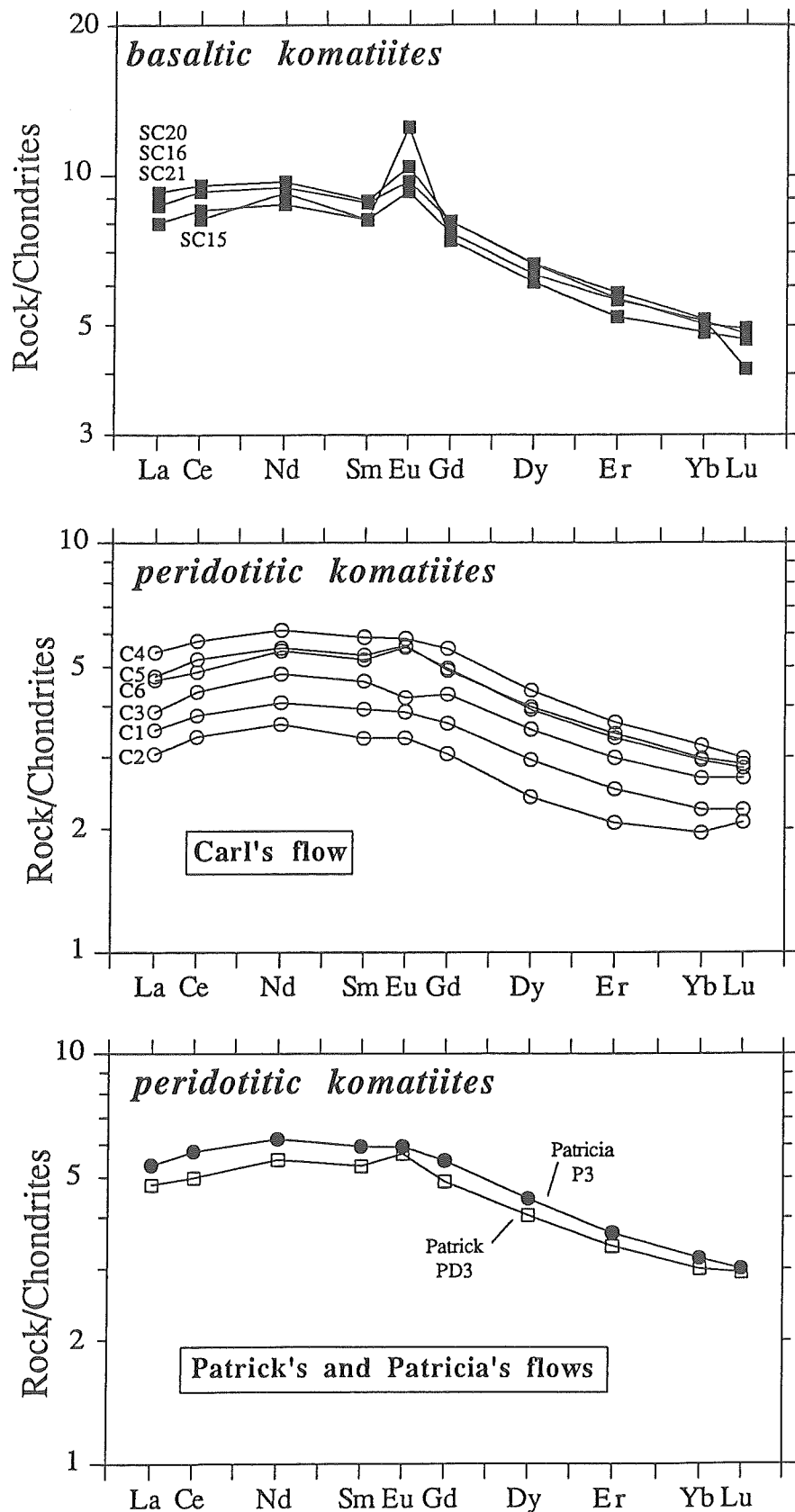


Figure 4: REE profiles. Normalizing values are from Gruau et al. (1990b).

Isotopic data

Neodymium

Sm-Nd isotopic ratios were measured on all the peridotitic komatiite samples and on basaltic komatiites SC20 and SC21 (Table 4). Three important points are to be noted:

1) All samples share nearly identical $^{147}\text{Sm}/^{144}\text{Nd}$ ratios (0.1800 to 0.1906; variation $\approx 6\%$) and $^{143}\text{Nd}/^{144}\text{Nd}$ ratios (0.512426 to 0.512603; variation $\approx 0.04\%$), which is not surprising in view of the uniform REE profiles.

2) T_{CHUR} model ages (Table 4) are extremely variable and unrealistically young (2540–550 Ma). T_{DM} model ages are also somewhat scattered, but the range is much smaller and the values make more geological sense. In fact, by pooling all the available data, a mean T_{DM} model age of 3530 ± 50 ($2s_m$) Ma is obtained, a result which is not significantly different from the zircon ages thought to represent the initial volcanic episode in the Onverwacht Group (3480–3450 Ma; Armstrong et al., 1990).

3) in Table 4, we list individual initial $e_{\text{Nd}}(T)$ values calculated using 3450 Ma as the age of magmatic crystallization. All samples (including the two basaltic komatiites) yield positive $e_{\text{Nd}}(3450)$ values, covering a narrow range around +2.5. Combining all the data, the mean $e_{\text{Nd}}(3450)$ value is $+2.4 \pm 0.2$ ($2s_m$). Assuming an age of 3480 Ma, the mean value is not significantly different: $+2.5 \pm 0.2$ (s_m).

Oxygen and Hydrogen

Oxygen and hydrogen isotopic data are listed in Table 5. In the basaltic komatiites, $d^{18}\text{O}$ values are nearly constant (from +4.8 to +5.0‰). In the peridotitic komatiites, $d^{18}\text{O}$ values are lower, and are also more variable (from +3.2 to +4.5‰). Comparison of Table 5 and Figure 2 shows that the variation of $d^{18}\text{O}$ values among peridotitic komatiites is a feature specific to each flow: ranges as well as absolute values of $d^{18}\text{O}$ are similar in the three flows, with the lowest values (+3.4‰ for Patricia's Flow; +3.3‰ for Patrick's Flow; +3.2‰ for Carl's Flow) being always observed in samples from the lower cumulate zone.

Amphibole separates (Mg-hornblende) from basaltic komatiites SC16, SC19 and SC20 gave identical $d^{18}\text{O}$ values, around +5.0‰; dD values are more variable, ranging from -77 to -88‰. The $d^{18}\text{O}$ value of SC16 magnetite separate is +0.1‰ (Table 5).

Argon

Argon isotope ratios obtained during the course of step-heating of amphiboles SC16 and SC19 are presented in Table 6, and the age spectra illustrated in Figure 5. $^{40}\text{Ar}/^{39}\text{Ar}$ results for amphibole SC19 yield a remarkably flat pattern with a plateau age of 2897 ± 16 Ma corresponding to 98% of the ^{39}Ar released (1050 to 1400°C). The age pattern for amphibole SC16 is not as flat, being saddle - shaped with low ages for low (<1150°C) and high (>1350°C) temperature steps. The plateau for amphibole SC16, where 75% of the ^{39}Ar is released between 1200 and 1350°C, yields an age of 2866 ± 15 Ma.

Table 4: Sm-Nd isotopic data for Schapenburg whole-rock samples

Sample N°	Sm (ppm) ^a	Nd (ppm) ^a	$^{147}\text{Sm}/^{144}\text{Nd}$ ^b	$^{147}\text{Sm}/^{144}\text{Nd}$	$^{143}\text{Nd}/^{144}\text{Nd}$	$2\sigma_{\text{m}}$	$\varepsilon_{\text{Nd}}(0)$ ^c	$\varepsilon_{\text{Nd}}(3450)$ ^c	$T_{\text{DM}}(\text{Ga})$ ^d	$T_{\text{CHUR}}(\text{Ga})$ ^c
<i>Carl's Flow</i>										
C1	0.787	2.524	0.1885	0.512575	18	-1.2±0.4	+2.5±0.5	3.51	1.17	
C2	0.672	2.228	0.1823	0.512421	20	-4.2±0.4	+2.2±0.5	3.56	2.29	
C3	0.964	3.077	0.1894	0.512562	19	-1.5±0.4	+1.8±0.5	3.72	1.58	
C4	1.159	3.712	0.1888	0.512571	24	-1.3±0.5	+2.3±0.6	3.57	1.29	
C5	1.021	3.297	0.1872	0.512531	17	-2.1±0.4	+2.2±0.5	3.59	1.72	
C6	1.011	3.254	0.1878	0.512574	18	-1.2±0.4	+2.7±0.5	3.42	1.10	
<i>Patricia's Flow</i>										
P1	0.643	2.110	0.1842	0.512475	29	-3.2±0.6	+2.4±0.7	3.51	1.99	
P2	0.992	3.230	0.1857	0.512482	16	-3.0±0.3	+1.9±0.4	3.65	2.15	
P3	1.099	3.570	0.1861	0.512533	14	-2.0±0.3	+2.7±0.4	3.43	1.51	
P4	1.085	3.516	0.1866	0.512549	19	-1.7±0.4	+2.8±0.5	3.40	1.34	
P5	1.070	3.440	0.1880	0.512549	19	-1.7±0.4	+2.2±0.5	3.56	1.56	
<i>Patrick's Flow</i>										
PD1	0.579	1.910	0.1833	0.512443	23	-3.8±0.5	+2.2±0.6	3.56	2.20	
PD2	1.148	3.844	0.1806	0.512441	13	-3.8±0.3	+3.4±0.4	3.27	1.85	
PD3	1.024	3.272	0.1892	0.512590	21	-0.9±0.4	+2.4±0.5	3.51	0.98	
PD4	1.227	3.891	0.1906	0.512616	25	-0.4±0.5	+2.3±0.6	3.56	0.55	
<i>Basaltic komatiites</i>										
SC20	1.725	5.794	0.1800	0.512358	20	-5.5±0.4	+2.0±0.5	3.59	2.54	
SC21	1.576	5.228	0.1822	0.512426	20	-4.1±0.4	+2.3±0.5	3.52	2.23	

a The error is ±2%

b The error on this ratio is ±0.2%

c Calculated using a $^{147}\text{Sm}/^{144}\text{Nd}$ ratio of 0.1967 and a $^{143}\text{Nd}/^{144}\text{Nd}$ ratio of 0.513638 for the present-day chondritic uniform reservoir (CHUR)

d Calculated using a $^{147}\text{Sm}/^{144}\text{Nd}$ ratio of 0.2137 and a $^{143}\text{Nd}/^{144}\text{Nd}$ ratio of 0.513150 for the present-day depleted mantle reservoir (DM)

Table 5: Oxygen and hydrogen isotopic data *

Sample N°	$\delta^{18}\text{O}$	δD
Whole-rocks		
<i>Patricia's flow</i>		
P 1	3.39±0.02	
P 2	3.95±0.02	
P 3	4.50±0.02	
P 4	4.46±0.05	
P 5	4.50±0.06	
<i>Patrick's flow</i>		
PD 1	3.25±0.05	
PD 2	4.48±0.02	
PD 3	4.03±0.08	
PD 4	4.33±0.02	
<i>Carl's flow</i>		
C 1	3.64±0.14	
C 2	3.21±0.03	
C 3	4.16±0.04	
C 4	4.57±0.09	
C 5	4.30±0.02	
C 6	4.39±0.13	
<i>Basaltic komatiites</i>		
SC 15	5.02±0.02	
SC 16	4.92±0.04	
SC 17	4.82±0.06	
SC 18	5.04±0.06	
SC 19	5.01±0.03	
SC 20	4.92±0.02	
SC 21	4.91±0.06	
SC 22	4.91±0.02	
SC 22	4.91±0.02	
Minerals		
<i>Mg-hornblende</i>		
SC 16	4.95±0.10	-76.8±0.8
SC 19	5.05±0.03	-87.7±1.0
SC 20	5.03±0.03	-80.8±0.1
<i>Magnetite</i>		
SC 16	0.08±0.05	

* The errors presented on both oxygen and hydrogen isotopic ratios correspond to the reproducibility of two to four separate extractions and mass spectrometry analyses. Total uncertainty with respect to the VSMOW scale is estimated to be lower than 0.1 to 0.15 ‰ (oxygen) and than 2‰ (hydrogen)

Table 6: Argon data

T (°C)	$^{40}\text{Ar}/^{39}\text{Ar}$	$^{36}\text{Ar}/^{39}\text{Ar} * 100$	$^{37}\text{Ar}/^{39}\text{Ar}$	$^{39}\text{Ar}/^{40}\text{Ar}$	% ^{39}Ar released	Age (Ma)	2σ
<i>SC19 Amphibole</i>							
500	0.0	63.8	12.94	0.577	0.3	0	0
600	22.1	27.6	0.0	0.971	0.4	578	43
700	643.8	45.5	42.45	0.146	0.4	4483	17
800	133.4	5.97	14.93	0.666	0.7	2143	15
1050	288.9	0.21	39.32	0.348	1.1	3213	15
1150	234.7	0.80	36.97	0.424	11.3	2907	14
1200	237.8	0.04	38.16	0.423	29.9	2926	14
1250	232.2	0.17	35.83	0.432	61.2	2891	14
1300	228.0	0.13	35.00	0.440	76.7	2865	14
1350	233.3	1.30	37.13	0.424	96.6	2898	14
1400	231.3	0.03	0.0	0.435	99.5	2886	14
1450	185.2	0.16	0.0	0.542	100.0	2573	14
<i>SC16 Amphibole</i>							
500	18.7	14.1	18.74	1.670	2.2	500	24
600	33.8	5.85	2.11	1.969	6.4	822	12
700	90.8	1.99	4.97	1.041	8.0	1689	12
800	119.0	16.9	10.19	0.595	9.6	2001	20
1000	106.6	8.54	16.36	0.763	11.0	1871	15
1150	158.4	2.95	53.54	0.602	18.1	2363	14
1200	228.0	0.80	61.70	0.437	29.1	2865	14
1250	217.6	1.73	61.97	0.452	42.7	2798	14
1300	225.3	0.14	63.25	0.446	67.2	2848	14
1350	236.4	0.00	67.71	0.426	93.2	2917	19
1400	105.6	0.02	36.27	0.953	96.0	1860	11
1450	40.1	-0.94	38.45	2.700	100.0	941	7

DISCUSSION

From the results presented above, a number of conclusions can be drawn:

- 1) both amphibole fractions analysed for their $^{40}\text{Ar}/^{39}\text{Ar}$ age spectrum give consistent results (Fig. 5). Because the closure temperature for Ar is high in amphibole ($\geq 600^\circ\text{C}$ for $> 200\text{mm Mg-hornblende}$; Berger and York, 1981) and appears to exceed the peak metamorphic conditions recorded by the samples (see below), the calculated plateau ages (2897 ± 16 Ma and 2866 ± 15 Ma) should represent the age of crystallization of the amphibole-bearing metamorphic assemblages, hence fixing the period of metamorphism in the SGR at around 2900 Ma ago. 2900 Ma corresponds to the eruption age of the Nsuze Group as well as to the intrusion age of the Usushwana Igneous Suite (2940 ± 22 Ma and 2871 ± 30 Ma, respectively; Hegner et al., 1984). A widespread 2900 Ma-old heat supply inducing metamorphic recrystallization may be coeval with these magmatic events. Although the existence of a thermal event at around 2900 Ma has long been recognized in the area south of the BGB (e.g. Barton et al., 1983), it was so far regarded as having played a minor role in the post formation history of the greenstones. Clearly, the present results require a partial reassessment of such a view point;

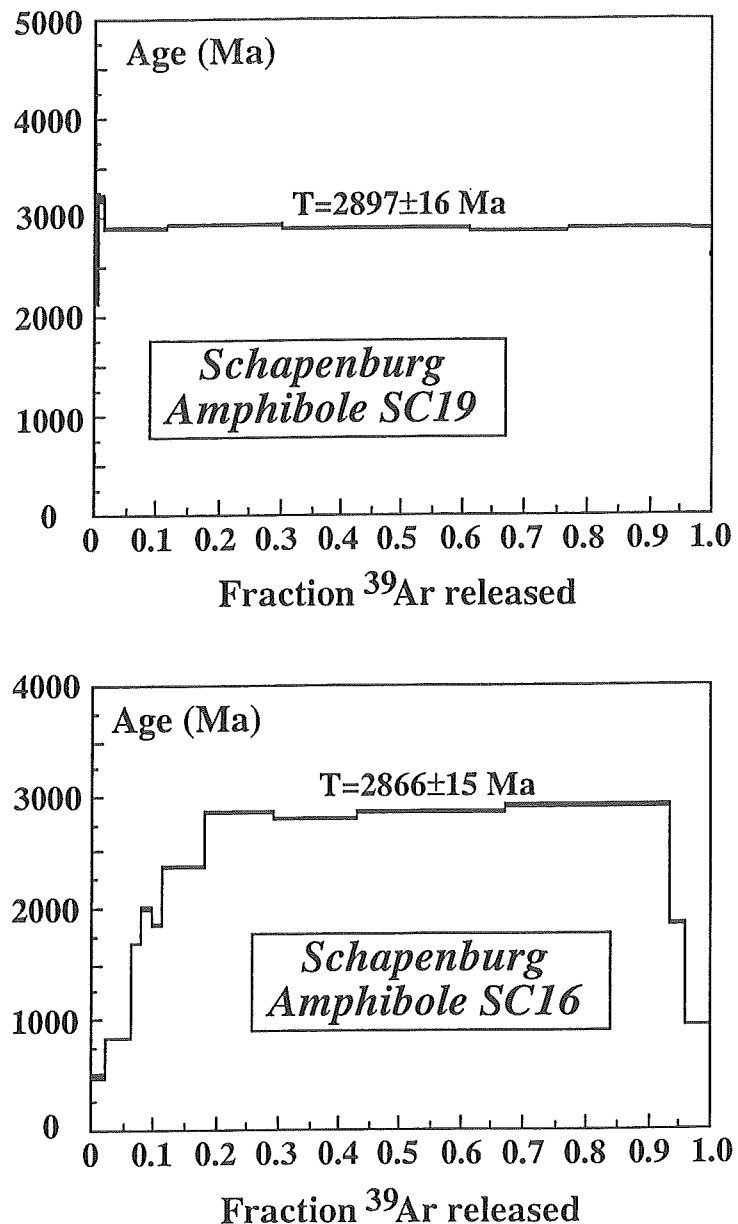


Figure 5: Argon age spectra. Vertical widths of the boxes represent 2s errors.

2) estimates of metamorphic temperature yield $450\pm50^\circ\text{C}$. The presence of antigorite, which has an upper stability temperature of $\approx 500^\circ\text{C}$ for a pressure of the order of 3Kb (Hemley et al., 1977), is consistent with thermometric calculations based on chemical fractionations observed among magnetite-ilmenite pairs ($T \approx 400^\circ\text{C}$, Table 2). One magnetite-amphibole pair gives an apparent metamorphic temperature of $460\pm20^\circ\text{C}$, using the magnetite-water and amphibole-water empirical fractionation coefficients of Bottinga and Javoy (1975). Our temperature estimates agree with the lower limit (500°C) of the temperature range obtained by Anhaeusser (1983) from his study of mineral parageneses;

3) the $d^{18}\text{O}$ values of the Schapenburg komatiites are all lower than the present-day

mantle reference values and/or the values found in modern unaltered sea-floor basalts ($+5.7 \pm 0.3\text{\textperthousand}$, Kyser, 1986, and references therein). $d^{18}\text{O}$ values for the Archaean mantle and related magmas are not as constrained as their present-day equivalents. However, isotopic study of the least altered komatiites or of magmatic minerals from spatially related basic-ultrabasic intrusions yield primary isotopic values not very different from those of modern mantle: $d^{18}\text{O} = +5.6$ to $+6.0\text{\textperthousand}$ (Hoefs and Binns, 1978; Beaty and Taylor, 1982; Smith et al., 1984). Thus, the oxygen isotopic compositions recorded in the komatiites from Schapenburg are not primary values: they likely result from some degree of isotopic exchange between the rocks and a fluid phase. From the $^{40}\text{Ar}/^{39}\text{Ar}$ isotopic results, it is postulated that this isotopic exchange corresponds to the metamorphic recrystallization event at around 2900 Ma;

4) from Table 3 and Figure 4, it is clear that Eu was mobile in Schapenburg greenstones. This is best illustrated by the variable and inconsistent Eu anomalies displayed by the peridotitic komatiite samples. Inconsistent Eu anomalies are common in many Archaean komatiites worldwide (including the well-preserved komatiite lava flows from Canada), which are thought to be due to the different behaviour of divalent Eu from other trivalent REE (Sun and Nesbitt, 1978; Jahn and Sun, 1979; Arndt, 1986b). By contrast, it appears that the other REE were not significantly fractionated during the evolution of these rocks. Let us consider Carl's Flow as an example: MgO concentrations range from 25.5 to 31.8% (Table 3), which suggests that low-pressure differentiation was controlled solely by olivine fractionation (Arndt, 1986b). Because the processes of olivine removal and accumulation cannot fractionate the REE (olivine/liquid partition coefficient are $<<1.0$ for all the REE; e.g. Fujimaki et al., 1984), both $(\text{La}/\text{Sm})_{\text{N}}$ and $(\text{Gd}/\text{Yb})_{\text{N}}$ ratios should remain constant from the bottom (olivine cumulate, high MgO and Ni contents) to the top of the flow (quenched liquid with lower MgO and Ni contents), which is basically what we observe in Carl's Flow (Table 3; Fig. 4). Moreover, an immobility of the REE as a group (except Eu) is suggested by the general decrease of REE abundances (for parallel patterns) with increasing MgO and Ni contents. Such a feature is common in fresh komatiites and result from olivine accumulation (Arndt, 1986b). Also, in the event of a significant REE redistribution on the scale of the whole-rock, there should be some relationships observed between the REE patterns and the secondary mineralogy (see Gruau et al., 1992). However, no such relationship exists in the present greenstone suite: samples with highly contrasted mineral proportions such as peridotitic komatiite C2 (serpentine $>70\%$) and basaltic komatiite SC16 (amphibole $\approx 95\%$) yield similar $(\text{La}/\text{Sm})_{\text{N}}$ and $(\text{Gd}/\text{Yb})_{\text{N}}$ ratios (Table 3; Fig. 4). Recent work carried out on the komatiites from Tipajajarvi and Kuhmo in eastern Finland (Tourpin et al., 1991; Gruau et al., 1992) and from Crixas in Brazil (Arndt et al., 1989), show that komatiites may experience partial to total resetting of their REE patterns during low- to medium-grade metamorphic recrystallization. Clearly, the Schapenburg rocks display the opposite type of behaviour: except for Eu, the pervasive low- to medium-grade metamorphic recrystallization did not significantly disturb the REE patterns; and

5) the Sm-Nd results also argue for REE immobility: as already pointed out, the T_{DM} model ages are equal within errors to the zircon ages which are thought to represent the eruption of the Lower Onverwacht Group volcanic rocks. Moreover, the uniformity of initial e_{Nd} values observed in Carl's, Patrick's and Patricia's Flows is to be expected for the different textural zones of komatiite flows erupted from a common parental magma. Judging

from the +2.5 initial $e_{Nd}(T)$ values, it is clear that the ultimate source(s) of Schapenburg komatiites was not primitive mantle, but a part of the mantle depleted in LREE.

Chemical and isotopic effect of serpentinization

The Schapenburg rocks did not behave as closed systems for all elements. Consider the distribution of $\text{CaO}/\text{Al}_2\text{O}_3$ and $\text{Al}_2\text{O}_3/\text{TiO}_2$ ratios across the peridotitic komatiite lava flows: both ratios should remain constant because olivine, the only fractionating phase, does not accommodate any of these three oxides. Yet, $\text{CaO}/\text{Al}_2\text{O}_3$ and $\text{Al}_2\text{O}_3/\text{TiO}_2$ are seen to cover a wide range in the komatiite lava flow samples (1.1-2.1, and 9.8-16.9, respectively; Table 3).

As can be seen in Figure 3, most of the variation of $\text{CaO}/\text{Al}_2\text{O}_3$ and $\text{Al}_2\text{O}_3/\text{TiO}_2$ ratios is in samples from the lower cumulate zones. By contrast, values in samples from the upper spinifex zones (quenched liquids) are close to those observed in the basaltic komatiites, hence corresponding to the average values of Al-depleted or Group II komatiites worldwide. It appears that the whole-rock chemistry is to some extent controlled by the modal composition of the secondary assemblages. Indeed, a major peculiarity of the cumulate zone samples is their high abundance in secondary serpentine (Table 1), which appears to exert some influence on $\text{CaO}/\text{Al}_2\text{O}_3$ and $\text{Al}_2\text{O}_3/\text{TiO}_2$ ratios: in the TiO_2 vs. MgO and CaO vs. MgO diagrams (Fig. 6), the compositions of cumulate zone samples with 70 % serpentine (e.g. C2 and P1) plot below olivine control lines. In turn, the high abundance of serpentine in the cumulate zone samples is itself a consequence of the high modal abundance of olivine in the primary paragenesis.

Elemental fluxes in the Schapenburg peridotitic komatiite flows cannot be properly evaluated because of the lack of primary mineral phases which would allow the calculation of volume and density changes. However, relative variations in elemental abundances can be evaluated. This is made possible by using CaO/Nd , TiO_2/Nd and $\text{Al}_2\text{O}_3/\text{Nd}$ ratios, for two reasons: 1) Nd behaved as an immobile element in all samples (see above); and 2) CaO/Nd , TiO_2/Nd and $\text{Al}_2\text{O}_3/\text{Nd}$ ratios are not fractionated by olivine addition or removal. Thus, the average CaO/Nd , TiO_2/Nd and $\text{Al}_2\text{O}_3/\text{Nd}$ ratios of the samples that plot on - or very close to - the olivine control lines in Figure 6 (spinifex zone samples) could be taken as the initial magmatic ratios, and used as reference values to estimate the direction and relative amplitude of elemental fluxes. This procedure is illustrated further on Figure 7, in which we report the vertical distributions of CaO/Nd , TiO_2/Nd and $\text{Al}_2\text{O}_3/\text{Nd}$ ratios in the three flows. Also shown in Figure 7 are the distributions of (1) Sr/Nd and $\text{Na}_2\text{O}/\text{Nd}$ ratios (2) whole-rock $d^{18}\text{O}$ values and (3) H_2O^+ concentrations. Four important points should be stressed:

1) In each of the cumulate zone flows, significant amounts of Ca and Ti were removed in some of the samples (particularly in sample C2), as inferred from the negative anomalies observed in the CaO/Nd and TiO_2/Nd ratio plots. By contrast, both CaO and TiO_2 appear to have been relatively immobile in samples from the upper spinifex-bearing zones;

2) Al was also mobile, but this element was added to certain samples, not lost. The location of Al mobility within the flows is different from that of Ca and Ti, i.e. at the base or the top of the flows.

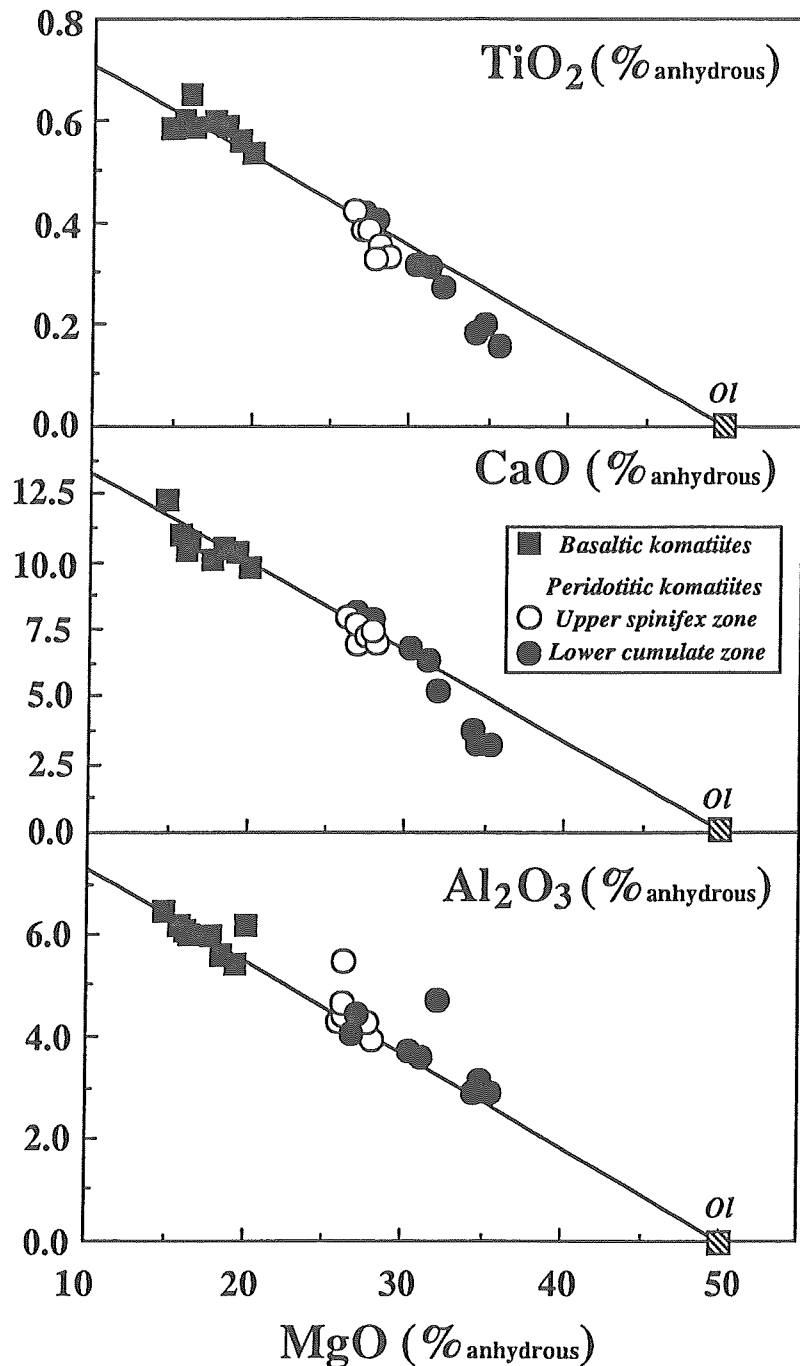


Figure 6: Variation diagrams. Olivine compositions (Ol) are from Arndt (1986).

3) profiles of Sr/Nd and $\text{Na}_2\text{O}/\text{Nd}$ contents are also marked by large negative anomalies in the lower parts of the three flows. The $\text{Na}_2\text{O}/\text{Nd}$, Sr/Nd and CaO/Nd profiles are closely similar to each other. The sensitivity of the lower cumulate zone samples to chemical alteration is also shown by the anomalously high Zr content of sample C2 (Table 3); and

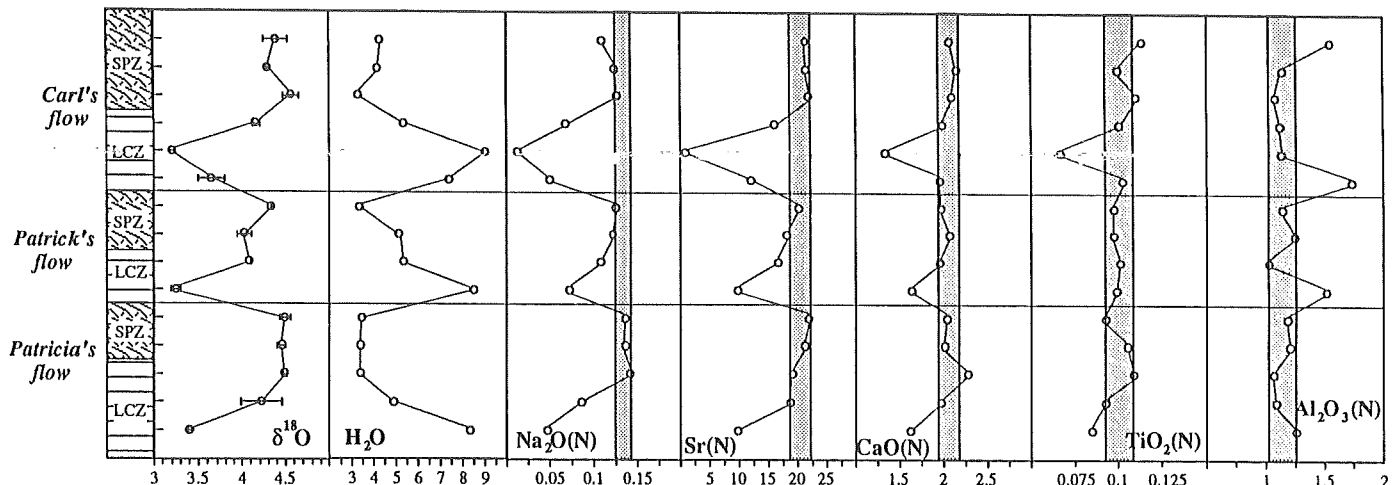


Figure 7: Diagram showing distribution of CaO/Nd , TiO_2/Nd , $\text{Al}_2\text{O}_3/\text{Nd}$, $\text{Na}_2\text{O}/\text{Nd}$ and Sr/Nd ratios in peridotitic komatiite samples as a function of their vertical position in the flow units, and comparison with distributions of whole-rock $\delta^{18}\text{O}$ values and H_2O^+ concentrations. The two lines in chemical profiles delineate maximum and minimum values of initial (magmatic) bulk flow rates. See text for further explanations.

4) finally, and most importantly, good correlations exist between the magnitude of elemental variations, the $\delta^{18}\text{O}$ values, and the degree of hydration (as inferred from L.O.I.). Moreover, the measured whole-rock oxygen isotopic compositions appear to be controlled by the secondary mineralogy since the $\delta^{18}\text{O}$ values of the Schapenburg greenstones are negatively correlated with the amount of serpentine in the rock (Fig. 8). Comparison of the extreme rock types, namely basaltic komatiites and lower cumulate zone samples, which more or less correspond to a binary mixture between amphibole and serpentine (\pm minor chlorite) demonstrates that serpentine is ^{18}O -depleted compared to coexisting amphibole in the SGR greenstones. This observation is compatible with natural mineral data available for similar metamorphic conditions. Beaty and Taylor (1982) deduced from their study of Abitibi komatiites that tremolite has a slightly higher $\delta^{18}\text{O}$ value than coexisting serpentine for temperatures close to 300°C . Wenner and Taylor (1973) analysed oceanic antigorites and found $\delta^{18}\text{O}$ values in the range $+2$ to $+4\text{\textperthousand}$ for temperatures exceeding 400°C and reacting fluids dominated by magmatic waters. Amphiboles with $\delta^{18}\text{O}$ values close to $+5\text{\textperthousand}$ were found in various rocks metamorphosed in the amphibolite facies or equilibrated with magmatic fluids (e.g. Garlick and Epstein, 1967; Agrinier et al., 1988).

The above correlations suggest that fluid-rock interaction was the main process determining the elemental variations as well as the $\delta^{18}\text{O}$ values of whole-rock samples.

Isotopic composition of the fluid phase

In order to evaluate the oxygen isotopic composition of the fluid present during the metamorphic recrystallization of the Schapenburg rocks, it is necessary to estimate the water/rock ratio. Indeed, the $\delta^{18}\text{O}$ value of the fluid in equilibrium with a given rock sample

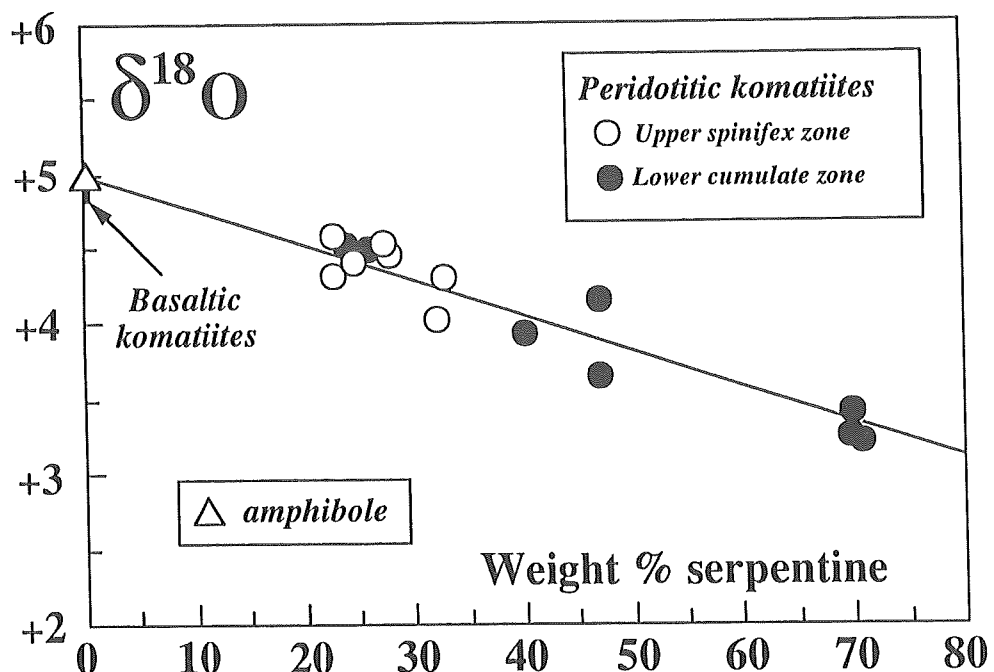


Figure 8: Diagram illustrating negative correlation between $d^{18}\text{O}$ values of whole-rock samples and the proportion of serpentine.

may be very different from the initial value if the water/rock ratio is small. For the following reasons, we argue that the fluid/rock ratio was high enough ($>>1$) to keep the $d^{18}\text{O}$ value of the fluid more or less constant during the interaction: 1) all the whole-rock samples yield $d^{18}\text{O}$ values lower than the mantle reference value, which indicates that the rock system did not behave as an infinite isotopic reservoir; 2) the low $d^{18}\text{O}$ values are buffered on a km-scale; and 3) the correlation of whole-rock $d^{18}\text{O}$ values with the proportions of secondary minerals (Fig. 8) suggests some kind of isotopic buffering by a pervasive fluid flux.

Using the equation for open-system exchange (Taylor, 1977) at 450°C, we obtain a $d^{18}\text{O}_{\text{fluid}}$ value in the range +5.5 to +7‰. $D_{\text{rock-water}}$ values were calculated from mineral proportions and the curves of Bottinga and Javoy (1975) for amphibole and magnetite, and Wenner and Taylor (1971) for serpentine. Using the fractionation equation of Suzuki and Epstein (1976), the hydrogen isotopic composition (dD) of water in equilibrium with magnesio-hornblende fractions is -65 to -50‰ (Table 5). These compositions are in the range found for Phanerozoic metamorphic or magmatic fluids (Sheppard et al., 1969; Boettcher and O'Neil, 1980; Sheppard, 1986); however, the possible range of dD values for such fluids during the Archaean is not known. By contrast, the $d^{18}\text{O}$ values of Archaean metamorphic fluids should be similar to modern values (rock-dominated systems). A magmatic origin for the Schapenburg metamorphic fluids is also compatible with the $d^{18}\text{O}$ values in the range +7 to +9‰ measured by TAYLOR (1977) in intrusive tonalitic and granitic plutons of the Barberton Mountain Land. The present data rule out the participation of surface-derived water (sea or meteoric water) unless they underwent strong exchange with the crust at high temperature prior to their interaction with the SGR.

CONCLUDING REMARKS

Preservation of primary chemical and isotopic signatures during metamorphic recrystallization

In contrast with certain other cases of metamorphosed komatiites (Arndt et al., 1989; Tourpin et al., 1991; Gruau et al., 1992), the metakomatiites from Schapenburg appear to have preserved most of their primary chemical and isotopic signatures during metamorphic recrystallization. With the exception of Eu, the REE were not significantly disturbed. Moreover, the values of CaO/Al₂O₃ and Al₂O₃/TiO₂ ratios which are crucial in determining the PT conditions of melting in the mantle source (see Herzberg, 1992), remained unchanged in a majority of samples (see above and Fig. 7). Despite the long interval of time between emplacement and metamorphism (≈ 600 Ma), $e_{Nd}(T)$ values are homogeneous throughout the whole magmatic suite, indicating that the Sm-Nd system was closed during metamorphism on the scale of the sample. The values we obtained for (Gd/Yb)_N, Al₂O₃/TiO₂ and CaO/Al₂O₃ ratios in the less altered samples (1.64 ± 0.06 (1s), 11 ± 1 (1s), and 1.8 ± 0.1 (1s), respectively) corroborate the values of Gruau et al. (1990a) and Herzberg (1992) for Barberton komatiites, which are considered as the most representative of Al-depleted komatiites. Nevertheless, it should be pointed out that these conclusions are only possible because the present study focused on individual lava flows. Non-systematic sampling, or sampling biased in favour of particular zones (e.g. sample C2), would not have furnished these elemental ratios.

Depleted versus undepleted mantle source

A second implication of this study concerns the composition of the mantle source and the nature of the melting process that formed the komatiites from Schapenburg. From the above Nd dataset it is clear that the ultimate mantle source of these greenstones was depleted in LREE ($e_{Nd}(T) \approx +2.5$), i.e. the source had a $^{147}\text{Sm}/^{144}\text{Nd}$ ratio higher than the chondritic reservoir. Taken on its own, this result has two important consequences: 1) given the fact that measured $^{147}\text{Sm}/^{144}\text{Nd}$ ratios are all lower than the chondritic value (Table 4), it confirms the hypothesis that garnet (majorite), with high Sm/Nd ratios, was a residual phase during the partial melting that formed these Al-depleted or Group II komatiites; only the presence of garnet in the solid residue could lead to simultaneous fractionation of the (Gd/Yb)_N, CaO/Al₂O₃, Al₂O₃/TiO₂, and $^{147}\text{Sm}/^{144}\text{Nd}$ ratios; and 2) It significantly modifies the accepted picture of Barberton komatiites tapping undepleted ($e_{Nd}(T) \approx 0$) mantle source regions (Hamilton et al., 1979; 1983; Gruau et al., 1990b).

The isotopic difference between Schapenburg komatiites ($e_{Nd}(T) \approx +2.5$) and the komatiites from the BGB ($e_{Nd}(T) \approx 0$) could reflect long-term heterogeneity of the early Archean mantle that lay beneath the Barberton Mountain Land. However, it should be noticed that none of the Nd isotopic studies so far carried out on BGB komatiites include analyses of samples from a single komatiite flow. In this context, the near-zero $e_{Nd}(T)$ values must be treated with caution. Recent studies (e.g. Tourpin et al., 1991; Gruau et al., 1992) show that it is only possible to interpret the initial Nd isotopic ratios of metakomatiites as primary (magmatic) isotopic memories after a *detailed study* of geochemical and isotopic variations in *single flow units*.

The Barberton Mountain Land: a window to the $d^{18}O$ value of the early Archaean ocean?

The final implication of this study concerns the use of $d^{18}O$ values from Barberton Mountain Land rocks to provide information on the isotopic composition of Archaean seawater. The $^{39}\text{Ar}/^{40}\text{Ar}$ ages now available for various metasedimentary and metavolcanic rocks of the BGB and surrounding greenstone remnants indicate the existence of discrete periods of thermal activity at 3480-3450, 3300-3200, 2900-2700 and 2100-2000 Ma (Lopez-Martinez et al., 1984, 1992; De Ronde et al., 1991; this study). Each period (except the 2100-2000 Ma event) *coincides with a major magmatic event* (Kamo and Davies, 1991). At Schapenburg, all record of possible interactions with Archaean seawater during emplacement of the volcanic rocks have been lost. The 2900 Ma magmatic activity south of the BGB and the consequent metamorphic recrystallization is likely the cause of this loss. On account of the rather general agreement between $^{39}\text{Ar}/^{40}\text{Ar}$ metamorphic ages and ages of magmatic activity, an important question arises: do any of the supracrustal lithologies from the Barberton Mountain Land preserve the isotopic record of their initial interaction with seawater?

As already mentioned, a property of metamorphic and/or magmatic fluids is to display rather constant oxygen isotope composition through time (rock-buffered fluid systems). Thus, the oxygen isotope compositions of the metamorphic and/or magmatic fluids which circulated at various epochs through the Barberton supracrustal rocks could have fluctuated only within a narrow range (a few d units). The intervention of magmatic/metamorphic fluids has been already isotopically documented in various sedimentary and volcanic rock units of the BGB. Smith et al. (1984) identified a significant "magmatic component" ($d^{18}O$ values around +5‰) in the fluid reacting with basalts and komatiites from the type section of the Komati Formation. Similar conclusions were drawn for the associated sediments of the Onverwacht Group. More precisely, Veizer et al. (1989a) concluded that the isotopic signatures of most carbonates coming from the Komati, Hooggenoeg and Kromberg Formations are hydrothermal ($d^{18}O$ of fluids around +6‰). They propose that "these hydrothermal waters were derived either from metamorphic dewatering at the base of the piles or from a magmatic source", and that they interacted with the supracrustals at temperatures in the range 200-500°C. Similarly, Knauth and Lowe (1978) studied a large number of chert samples from different parts of the Onverwacht Group. Although the highest values recorded by the cherts ($d^{18}O$ close to +22‰) were interpreted as evidence for a hot (70°C) Archaean ocean ($d^{18}O=0$ hypothesis), these authors admitted that some of the lower values (especially those down to +9‰) were problematic and likely resulted from interactions with metamorphic waters. Robert (1988) also found evidence for post-formation isotopic disturbances of the C (kerogen fraction) and oxygen isotopic ratios in cherts from the Onverwacht Group. Moreover, Weis and Wasserburg (1987) demonstrated from Rb-Sr systematics that the Onverwacht Group cherts "were all produced by a metamorphic or hydrothermal process which replaced and/or at least recrystallized the protolith". This event was dated at approximately 2100-2200 Ma, which is much later than the formation age.

Assuming that the carbonates and cherts from the BGB initially had initial $d^{18}O$ values similar to those of Phanerozoic (fresh) marine carbonates and cherts (i.e. ≈0‰ PDB and +32‰ SMOW, respectively), it is possible that their variable measured oxygen isotopic

compositions have arisen because these sediments subsequently exchanged with a fluid phase of metamorphic-magmatic origin ($\delta^{18}\text{O} \approx +6.0\text{\textperthousand}$), at various temperatures and under different water/rock ratio conditions. We have tested this possibility. The results are presented in Figure 9. It is a striking fact that, apart from those cherts and carbonates with $\delta^{18}\text{O}$ values around $+23\text{\textperthousand}$ (SMOW) and $-7\text{\textperthousand}$ (PDB), respectively, the oxygen isotopic compositions of all BGB chemical sediments can be explained in such a way. This requires water/rock ratios and exchange temperatures in the range 0.5-5.0 and 200-500°C, respectively. A 200-500°C temperature range corresponds to the widespread greenschist to lower amphibolite facies metamorphic conditions observed in the BGB (e.g. Veizer et al., 1989a).

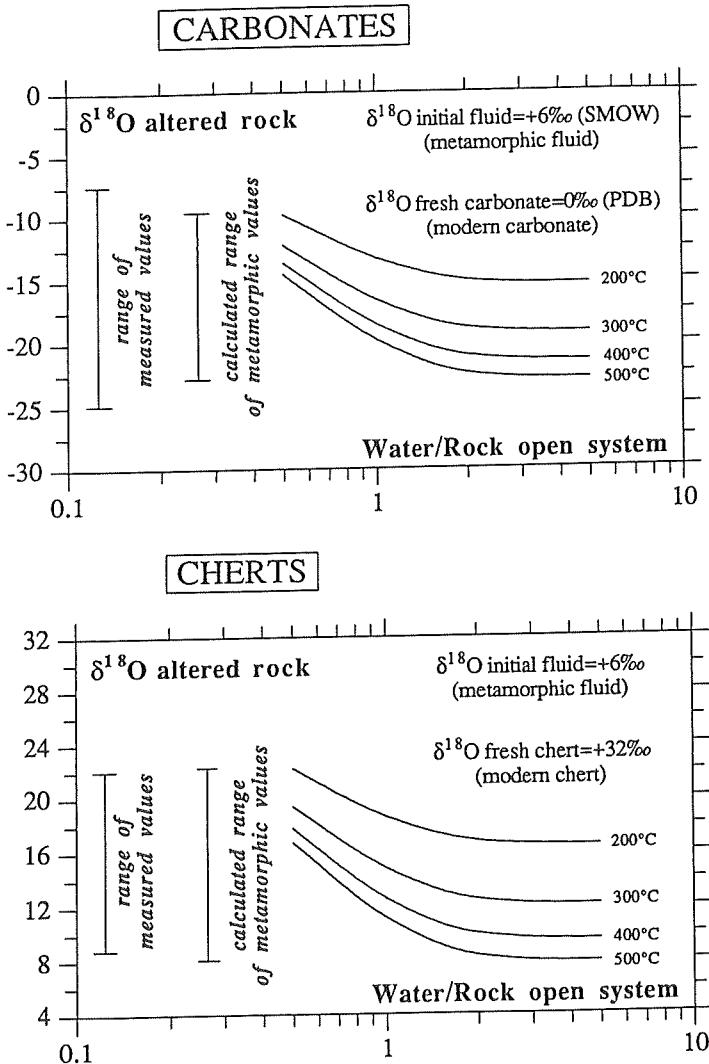


Figure 9: Diagram showing variations of $\delta^{18}\text{O}$ values in Barberton carbonates and cherts and comparison with the values calculated assuming isotopic exchange between Phanerozoic (fresh) marine carbonates and cherts and a fluid of metamorphic-magmatic origin ($\delta^{18}\text{O}$ around $+6\text{\textperthousand}$). Good fit arises between measured and calculated values when exchange temperatures and water/rock ratio conditions are in the range 200-500°C and 0.5-5.0 respectively. The curves were calculated using the isotopic fractionation factors of O'Neil et al. (1969) - carbonates - and Knauth and Epstein (1976) - cherts. The isotopic ratios are reported relative to PDB (carbonates) and SMOW (cherts). Data sources: Veizer et al. (1989a) and Knauth and Lowe (1978). $d^{18}\text{O}$ (SMOW) = $1.03086(d^{18}\text{O}(\text{PDB})) + 30.86$ (Friedman and O'Neil, 1977).

ACKNOWLEDGEMENTS

C. Lécuyer is very grateful to J.R. O'Neil for providing access to the University of Michigan analytical facilities. We are also indebted to H. Maluski, who provided the Ar age data, as well as to F. Martineau, N. Morin and J. Macé for their assistance during work carried out at the University of Rennes. This paper benefited by critical comments and suggestions from N.T. Arndt, T.K. Kyser, J. Ludden and D.W. Mittlefehldt. Dr. M. S. N. Carpenter assisted with the final presentation of the paper.

REFERENCES

- AGRINIER P., JAVOY M. and GIRARDEAU J. (1988). Hydrothermal activity in a peculiar oceanic ridge: oxygen and hydrogen isotope evidence in the Xigaze ophiolite (Tibet, China). *Chem. Geol.*, **71**, 313-335.
- ANHAEUSSER C. R. (1980) A geological investigation of the Archaean granite-greenstone terrane south of the Boesmanskop syenite pluton, Barberton Mountain Land. *Trans. geol. Soc. S. Afr.*, **83**, 73-106.
- ANHAEUSSER C. R. (1983) The geology of the Schapenburg greenstone remnant and surrounding Archaean granitic terrane south of Badplass, Eastern Transvaal. *Spec. Publ. geol. Soc. S. Afr.* **9**, 31-44.
- ANHAEUSSER C.R. (1991). Schapenburg greenstone remnant. In: *Two Cratons and an Orogen - Excursion Guidebook and Review Articles for a Field Workshop Through Selected Archaean Terranes of Swaziland, South Africa and Zimbabwe* (ed. L. D. Ashwal), pp. 107-115. IGCP 280, Dept. of Geology, Univ. Witwatersrand, Johannesburg.
- ANHAEUSSER C. R. and ROBB L. J. (1980). Regional and detailed field and geochemical studies of Archaean trondhjemite gneisses, migmatites and greenstone xenoliths in the southern part of the Barberton Mountain Land, South Africa. *Precambrian Res.*, **11**, 373-397.
- ANHAEUSSER C. R. and ROBB L. J. (1981). Magmatic cycles and the evolution of the Archaean granitic crust in the eastern Transvaal and Swaziland. *Spec. Publ. geol. Soc. Aust.*, **7**, 457-467.
- ARMSTRONG R. A., COMPSTON W., DE WIT M. J. and WILLIAMS I. S. (1990). The stratigraphy of the 3.5-3.2 Ga Barberton Greenstone Belt revisited: a single zircon ion microprobe study. *Earth Planet. Sci. Lett.* **101**, 90-106.
- ARNDT N.T. (1986a). Komatiites: a dirty window to the Archean mantle. *Terra Cognita* **6**, 59-66.
- ARNDT N. T. (1986b). Differentiation of komatiite flows. *J. Petrol.*, **27**, 279-301.

- ARNDT N. T., TEIXEIRA N. A. and WHITE W. M. (1989). Bizarre geochemistry of komatiites from the Crixas greenstone belt, Brazil. *Contrib. Mineral. Petrol.* **101**, 187-197.
- BARTON J. M., ROBB L. J., ANHAEUSSER C. R. and VAN NIEROP D. A. (1983). Geochronologic and Sr-isotopic studies of certain units in the Barberton granite-greenstone terrane, South Africa. *Spec. Publ. Geol. Soc. S. Afr.*, **9**, 63-72.
- BAYLISS P. (1975). Nomenclature of the trioctahedral chlorites. *Canadian Mineral.*, **13**, 178-180.
- BEATY D. W. and TAYLOR H. P. J. (1982). The oxygen isotope geochemistry of komatiites: evidence for water-rock interaction. In *Komatiites* (ed. N. T. ARNDT and E. G. NISBET), pp. 267-280. George Allen and Unwin, London.
- BERGER G. W. and YORK D. (1981). Geothermometry from $^{40}\text{Ar}/^{39}\text{Ar}$ dating experiments. *Geochim. Cosmochim. Acta*, **43**, 795-811.
- BOETTCHERA. L. and O'NEIL J. R. (1980). Stable isotope, chemical and petrographic studies of high pressure amphiboles and micas: evidence for metasomatism in the mantle source regions of alkali basalts and kimberlites. *Amer. J. Sci.* **280A**, 594-621.
- BOTTINGA Y. and JAVOY M. (1975). Oxygen isotope partitioning among the minerals in igneous and metamorphic rocks. *Rev. Geophys. Space Phys.*, **13**, 401-418.
- BRYAN W. B., FINGER L. W. and CHAYES F. (1969). Estimating proportions in petrographic mixing equations by least-squares approximation. *Science*, **163**, 926-927.
- CLAYTON R. N. and MAYEDA T. K. (1963). The use of bromine pentafluoride in the extraction of oxygen from oxides and silicates for isotopic analyses. *Geochim. Cosmochim. Acta* **27**, 43-52.
- CLOETE M. (1991). An overview of metamorphism in the Barberton Greenstone Belt. In *Two Cratons and an Orogen - Excursion Guidebook and Review Articles for a Field Workshop through Selected Archaean Terranes of Swaziland, South Africa and Zimbabwe* (ed. L. D. Ashwal), pp. 84-98. IGCP 280, Dept. of Geology, Univ. Witwatersrand, Johannesburg.
- DAVIES R. D., ALLSOPP H. L., ERLANK A. J. and MANTON W. I. (1970). Sr-isotope studies on various layered mafic intrusions in southern Africa. *Spec. Publ. geol. Soc. S. Afr.*, **1**, 576-593.
- DEPAOLO D. J. and WASSERBURG G. J. (1976). Inferences about magma sources and mantle structure from $^{143}\text{Nd}/^{144}\text{Nd}$. *Geophys. Res. Lett.* **3**, 743-746.

- DERONDE C. E. J., HALL C. M., YORK D. and SPOONER E. T. C. (1991). Laser step-heating $^{40}\text{Ar}/^{39}\text{Ar}$ age spectra from early Archean ($\approx 3.5\text{ Ga}$) Barberton greenstone belt sediments: A technique for detecting cryptic tectono-thermal events. *Geochim. Cosmochim. Acta* **55**, 1933-1951.
- ERNST W. G. (1983). Mineral parageneses in metamorphic rocks exposed along tailuko Gorge, Central Mountain range, Taiwan. *J. metamorphic Geol.*, **1**, 305-329.
- FRIEDMAN I. and O'NEIL J. R. (1977). Compilation of stable isotope fractionation factors of geochemical interest. In *Data of Geochemistry*, 6th Ed (ed. M. Fleischer), U.S. Govt. Printing Office, Washington, D.C.
- FUJIMAKI H., TATSUMOTO M. and AOKI K. (1984). Partition coefficients of Hf, Zr and REE between phenocrysts and groundmass. *J. Geophys. Res.*, **89**, 662-672.
- GARLICK G. D. and EPSTEIN S. (1967). Oxygen isotope ratios in coexisting minerals of regionally metamorphosed rocks. *Geochim. Cosmochim. Acta*, **31**, 181-214.
- GRUAU G., CHAUVEL C., ARNDT N. T. and CORNICHET J. (1990a). Aluminum depletion in komatiites and garnet fractionation in the early Archean mantle: hafnium isotopic constraints. *Geochim. Cosmochim. Acta* **54**, 3095-3101.
- GRUAU G., CHAUVEL C. and JAHN B. M. (1990b). Anomalous Sm-Nd ages for the early Onverwacht Group volcanics: significance and petrogenetic implications. *Contrib. Mineral. Petrol.*, **104**, 27-34.
- GRUAU G., JAHN B. M., GLIKSON A. Y., DAVY R., HICKMAN A. H. and CHAUVEL C. (1987). Age of the Archean Talga-Talga Subgroup, Pilbara block, western Australia, and early evolution of the mantle: new Sm-Nd isotopic evidence. *Earth Planet. Sci. Lett.*, **85**, 105-116.
- GRUAU G., TOURPIN S., FOURCADE S. and BLAIS S. (1992). Loss of isotopic (Nd, O) and chemical (REE) memories during metamorphism of komatiites: new evidence from eastern Finland. *Contrib. Mineral. Petrol.*, **112**, 66-82.
- HAMILTON P. J., EVENSEN N. M., O'NIIONS R. K., SMITH H. S. and ERLANK A. J. (1979). Sm-Nd dating of Onverwacht Group volcanics, southern Africa. *Nature*, **279**, 298-300.
- HAMILTON P. J., O'NIIONS R. K., BRIDGWATER D. and NUTMAN A. (1983). Sm-Nd studies of Archaean metasediments and metavolcanics from West Greenland and their implications for the Earth's early history. *Earth Planet. Sci. Lett.*, **62**, 263-272.
- HEGNER E., KRÖNER A. and HOFMAN A.W. (1984). Age and isotope geochemistry of the Archaean Pongola and Usushwana suites in Swaziland, southern Africa: a case for crustal contamination of mantle-derived magma. *Earth Planet. Sci. Lett.*, **70**, 267-279.

- HEMLEY J. J., MONTOYA J. W., SHAW D. R. and LUCE R. W. (1977). Mineral equilibria in the MgO-SiO₂-H₂O system: II. Talc-antigorite-forsterite-anthophyllite-enstatite stability relations and some geologic implications in the system. *Amer. J. Sci.* **277**, 353-383.
- HERZBERG C. (1992). Depth and degree of melting of komatiites. *J. Geophys. Res.*, **97**, 4521-4540.
- HOEFS J. and BINNS R. A. (1978). Oxygen isotope compositions in Archean rocks from Western Australia, with special reference to komatiites. *USGS Open-file Rep.*, **78-701**, 180-182.
- HOFFMAN S. E., WILSON M. and STAKES D. S. (1986). Inferred oxygen isotope profile of Archaean oceanic crust, Onverwacht Group, South Africa. *Nature*, **321**, 55-58.
- JACOBSEN S. B. and WASSERBURG G. J. (1980). Sm-Nd isotopic evolution of chondrites. *Earth Planet. Sci. Lett.* **50**, 139-155.
- JAHN B. M. and SUN S. S. (1979). Trace element distribution and isotopic composition of Archean greenstones. In: *Origin and Distribution of the Elements* (ed. L. H. Ahrens), pp. 597-618. Pergamon Press, Oxford.
- JAHN B. M., GRUAU G. and GLIKSON A. Y. (1982). Komatiites of the Onverwacht Group, S. Africa: REE geochemistry and mantle evolution. *Contrib. Mineral. Petrol.*, **80**, 25-40.
- KAMO S. and DAVIS D. (1991). A review of geochronology from the Barberton Mountain Land. In: *Two Cratons and an Orogen - Excursion Guidebook and Review Articles for a Field Workshop Through Selected Archaean Terranes of Swaziland, South Africa and Zimbabwe* (ed. L. D. Ashwal), pp. 59-68. IGCP Project 280, Dept. of Geology, Univ. Witwatersrand, Johannesburg.
- KARHU J. and EPSTEIN S. (1986). The implication of the oxygen isotope records in coexisting cherts and phosphates. *Geochim. Cosmochim. Acta*, **50**, 1745-1756.
- KENDALL C. and COPLEN T. B. (1985). Multisample conversion of water to hydrogen by zinc for stable isotope determination. *Anal. Chem.*, **57**, 1437-1440.
- KNAUTH L. P. and EPSTEIN S. (1976). Hydrogen and oxygen isotope ratios in nodular and bedded cherts. *Geochim. Cosmochim. Acta*, **40**, 1095-1108.
- KNAUTH L. P. and LOWE D. R. (1978). Oxygen isotope geochemistry of cherts from the Onverwacht Group (3.4 billion years), Transvaal, South Africa, with implications for secular variations in the isotopic composition of cherts. *Earth Planet. Sci. Lett.*, **41**, 209-222.

- KRÖNER A. and TODT W. (1988). Single zircon dating constraining the maximum age of the Barberton greenstone belt, southern Africa. *J. Geophys. Res.*, **93**, 15329-15337.
- KYSER T. K. (1986). Stable isotope variations in the mantle. In *Stable isotopes in high temperature geological processes* (ed. J. W. Valley et al.); *Rev. Mineral.*, **16**, 141-164.
- LAIRD J. (1988). Chlorites: metamorphic petrology. In: *Hydrous Phyllosilicates (Exclusive of Micas)* (ed. S. W. Bailey); *Rev. Mineral.*, **19**, 405-453.
- LEAKE B. E. (1978). Nomenclature of amphiboles. *Amer. Mineral.*, **63**, 1023-1059.
- LOPEZ-MARTINEZ M., YORK D., HALL C. M. and HANES J. A. (1984). Oldest reliable $^{40}\text{Ar}/^{39}\text{Ar}$ ages for terrestrial rocks: Barberton Mountain komatiites. *Nature*, **307**, 352-355.
- LOPEZ-MARTINEZ M., YORK D. and HANES J. A. (1992). A $^{40}\text{Ar}/^{39}\text{Ar}$ geochronological study of komatiites and komatiitic basalts from the lower Onverwacht volcanics: Barberton Mountain Land, South Africa. *Precambrian Res.*, **57**, 91-119.
- MÉVEL C. (1984). Le métamorphisme dans la croute océanique. Apport de la Pétrologie à la compréhension des phénomènes de circulation hydrothermale (exemples dans l'Atlantique). Thèse Doctorat ès-Sciences Univ. Pierre et Marie Curie, 434.
- MONIÉ P., CABY R. and MALUSKI H. (1984). $^{40}\text{Ar}/^{39}\text{Ar}$ investigations within the Grande-Kabylie massif (northern Algeria): evidences for its Alpine structuration. *Eclogae Geol. Helv.*, **77**, 115-141.
- O'NEIL J. R., CLAYTON R. N. and MAYEDA T. K. (1969). Oxygen isotope fractionation in divalent metal carbonates. *J. Chem. Phys.*, **51**, 5547-5558.
- ROBERT F. (1988). Carbon and oxygen isotope variations in Precambrian cherts. *Geochim. Cosmochim. Acta*, **52**, 1473-1478.
- SHEPPARD S. M. F. (1986). Characterization and isotopic variations in natural waters. In: *Reviews in Mineralogy, Stable Isotopes in High Temperature Geological Processes* (ed. J.W. Valley et al.); *Rev. Mineral.*, **16**, 165-183.
- SHEPPARD S. M. F., NIELSEN R. L. and TAYLOR H. P. (1969). Oxygen and hydrogen isotope ratios of clay minerals from porphyry deposits. *Econ. Geol.*, **64**, 755-777.
- SMITH A. D. and LUDDEN J. N. (1989). Nd isotopic evolution of the Precambrian mantle. *Earth Planet. Sci. Lett.*, **93**, 14-22.

- SMITH H. S., O'NEIL J. R. and ERLANK A. J. (1984). Oxygen isotope compositions of minerals and rocks and chemical alteration patterns in pillow lavas from the Barberton greenstone belt, South Africa. In: *Archean Geochemistry* (ed. A. Kröner et al.), pp. 115-137, Springer-Verlag, New York.
- SUN S. S. and NESBITT R. W. (1978). Petrogenesis of Archean ultrabasic and basic volcanics: Evidence from rare earth elements. *Contrib. Mineral Petrol.*, **65**, 301-325.
- SUZUOKI T. and EPSTEIN S. (1976). Hydrogen isotope fractionation between OH-bearing minerals and water. *Geochim. Cosmochim. Acta*, **40**, 1229-1240.
- TAYLOR H. P. J. (1977). Water/rock interactions and the origin of H₂O in granitic batholiths. *J. Geol. Soc. London*, **133**, 509-558.
- TOURPIN S., GRUAU G., BLAIS S. and FOURCADE S. (1991). Resetting of REE, and Nd and Sr isotopes during carbonitization of a komatiite flow from Finland. *Chem. Geol.*, **90**, 15-29.
- VEIZER J., HOEFS J., LOWE D. R. and THURSTON P. C. (1989a). Geochemistry of Precambrian carbonates: II. Archean greenstone belts and Archean sea water. *Geochim. Cosmochim. Acta*, **53**, 859-871.
- VEIZER J., HOEFS J., RIDLER R. H., JENSEN L. S. and LOWE D. R. (1989b). Geochemistry of Precambrian carbonates: I. Archean hydrothermal systems. *Geochim. Cosmochim. Acta*, **53**, 845-857.
- VILJOEN M. J. and VILJOEN R. P. (1969a). The effects of metamorphism and serpentinization on the volcanic and associated rocks of the Barberton region. *Spec. publ. geol. Soc. S.Afr.*, **2**, 29-53.
- VILJOEN M. J. and VILJOEN R. P. (1969b). The geology and geochemistry of the lower ultramafic unit of the Onverwacht Group and a proposed new class of igneous rocks. *Spec. Publ. geol. Soc. S. Afr.*, **2**, 55-85.
- WEIS D. and WASSERBURG G. J. (1987). Rb-Sr and Sm-Nd isotope geochemistry and chronology of cherts from the Onverwacht Group (3.5 AE), South Africa. *Geochim. Cosmochim. Acta*, **51**, 973-984.
- WENNER D. B. and TAYLOR H. P., Jr. (1971). Temperatures of serpentinization of ultramafic rocks based on ¹⁸O/¹⁶O fractionation between coexisting serpentine and magnetite. *Contrib. Mineral. Petrol.*, **32**, 165-185.
- WENNER D. B. and TAYLOR H. P., Jr. (1973). Oxygen and hydrogen isotope studies of the serpentinization of ultramafic rocks in oceanic environments and continental ophiolite complexes. *Amer. J. Sci.*, **273**, 207-239.